臺灣醫用迴旋加速器學會
Taiwanese Society of Medical Cyclotron

中華民國核醫學學會
Society of Nuclear Medicine, Taiwan (R.O.C)

藥物動力學與全身分布影像試驗

林昆儒
林口長庚核醫科暨分子影像中心

2020-08-30 109年度學術推廣教育

(109年度科技部補助全國性學術團體辦理學術推廣業務計畫，**MOST 109-2312-B-A21-001**

目錄

- 定義，生物分布提供什麼資訊
- 生物分布實驗的工具，如何定量
- 動物人體活體實驗
- 新藥開發注意事項
- 個人化醫療

參考資料

Michael G. Stabin, PhD
Associate Professor, Department of Radiology/Radiological Sciences, Vanderbilt University, Nashville, Tennessee, USA

Fundamentals of Nuclear Medicine Dosimetry

Component

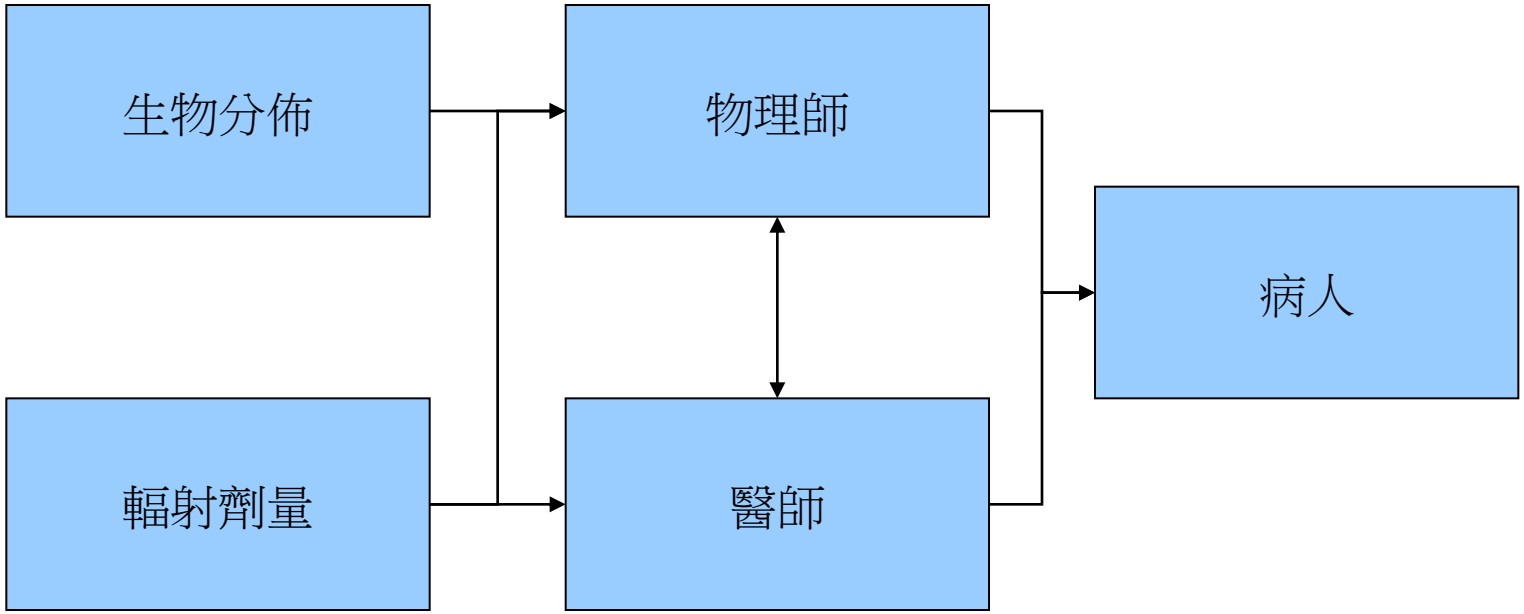

1. 定義

- 全身分布 Whole body distribution
  - 描述放射藥物進到體內後的全身分布情形
- 藥物動力學 Pharmacokinetics (PK)
  - 描述隨著時間藥物在進到生物體內的狀況，特別是從血液中的清除 clearance from blood ，或是初級代謝 first pass metabolism

2. 我們從生物分佈得到什麼資訊?

- 輻射劑量學
  - 提供輻射劑量計算，作為新藥申請資料
- 診斷評估
  - 放射追蹤劑的分佈對不對，正不正常，有無疾病
- 治療評估
  - 放射標記的藥物累積在標靶病理組織，評估劑量與治療效果
- 毒理評估
  - 放射標記的毒物累積在什麼器官，可能致病機轉

Pathophysiology

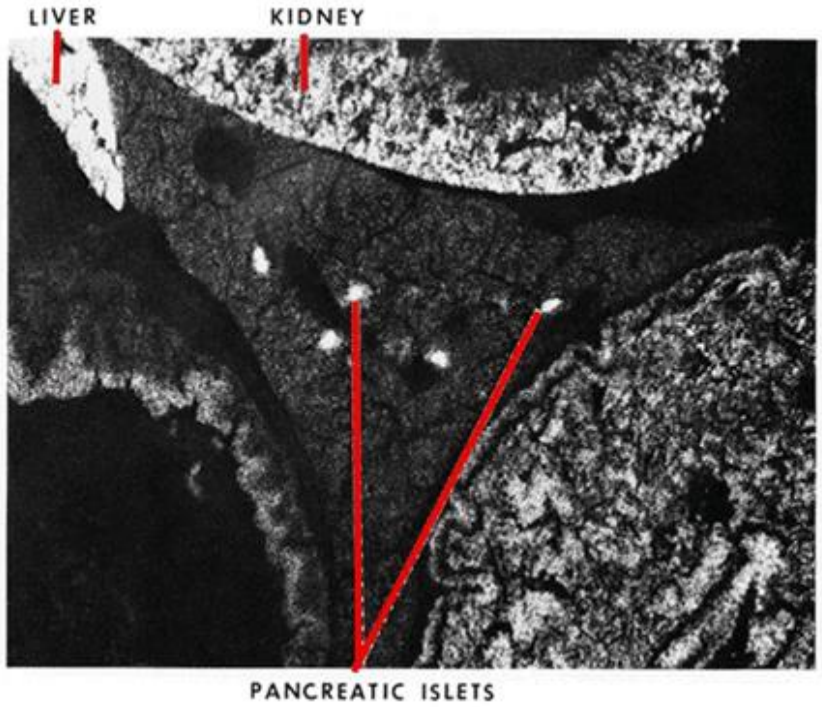

J. Endocrinol., 69, 455, 1976
Biochem J. 1974 September; 142(3): 673–683.

Detail of a whole-body from a mouse 4 hr after injection of ^{14}C-streptozotocin.

- **A high accumulation is present in the *pancreatic islets*. Streptozotocin as well as alloxan are accumulated in the pancreatic islets.**
- **The possible occurence of diabetogenic compounds in our environment may be a factor to consider in the evaluation of the etiology of diabetes mellitus in addition to inheritance.**
- **Streptozotocin is approved by the U.S. Food and Drug Administration (FDA) for treating metastatic cancer of the pancreatic islet cells.**

Toxin distribution

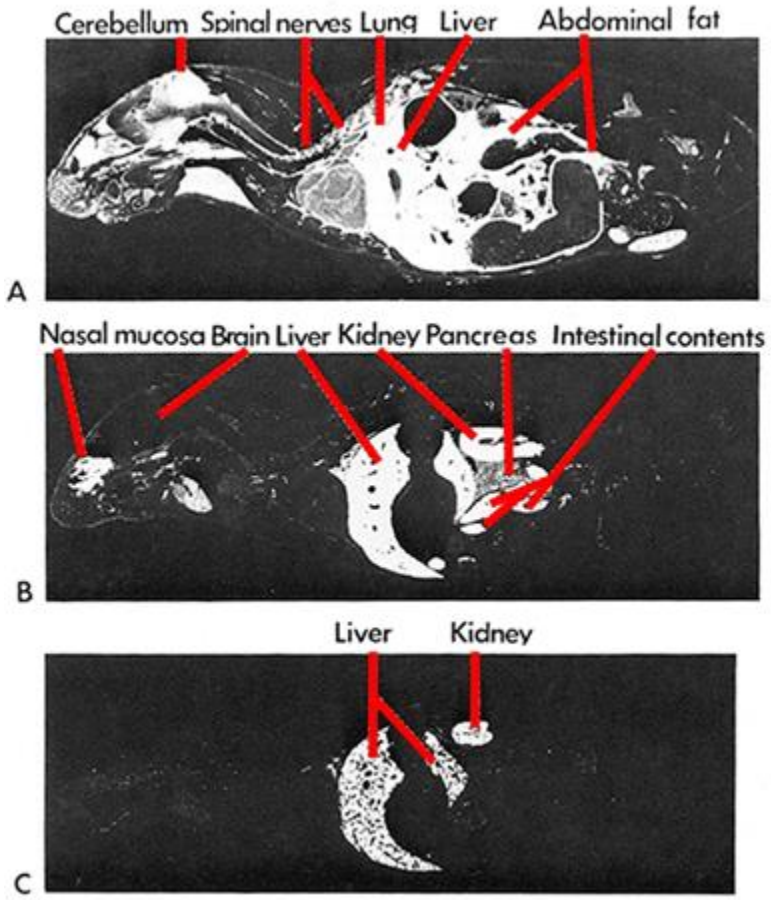

Whole-body autoradiograms of mice 2 hr after inhalation of 5 µl 14C-chloroform for 10 min.

A. **Hemisection exposed at -80o C. Note the high level of nonmetabolized chloroform in the cerebellum, spinal nerves, and meninges.**

B. **Dried, evaporated section. Nonvolatile metabolites are present in the liver, kidney, and the nasal mucosa.**

C. **(C): Dried, evaporated and extracted section. Note the irregular distribution of firmly bound raioactivity within the liver and the kidney.**

From Glenn, H. J. and Colombetti, L. G., Eds. Biologic Applications of Radiotracers. CRC Press, Inc., Boca Raton, Fl, 1982: 88-89. Previously from Bergman, K., Scand. J Work, Environ. Health,, 5 (Suppl.1), 1979

New drug distribution

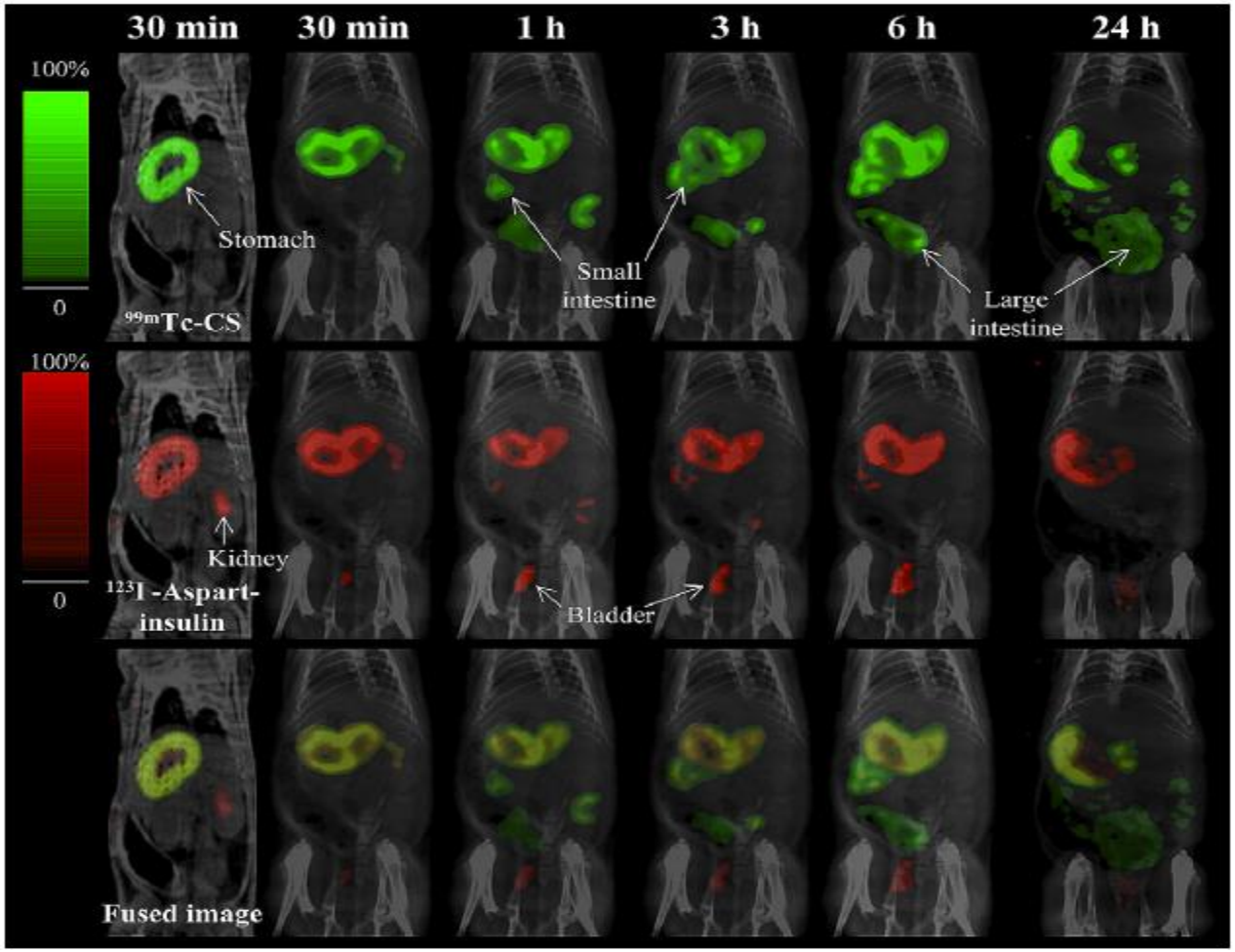

Diagnosis

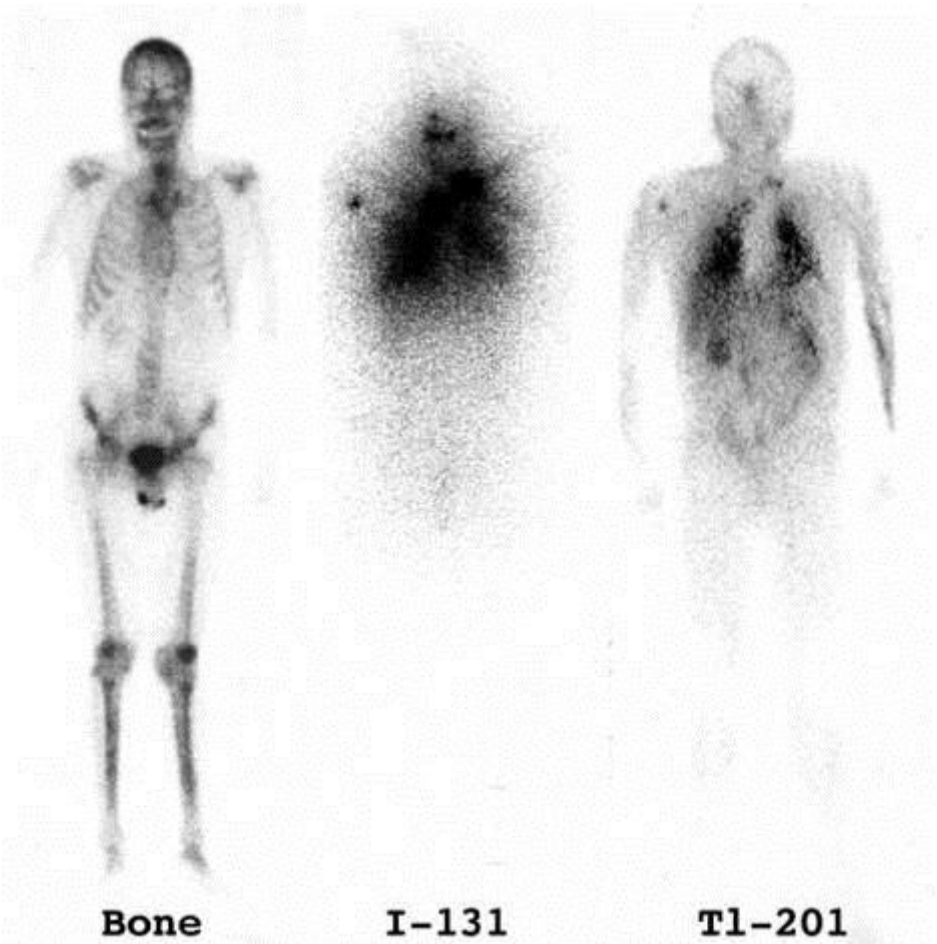

3.求得生物分佈的工具

- **Tissue dissection and counting**
- **Autoradiography**
- **Planar scintigraphy**
- **SPECT scanner**
- **PET scanner**

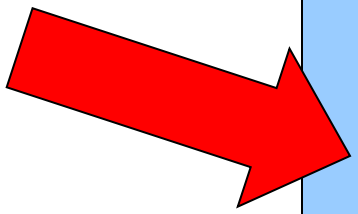

- ADME – human dosimetry
- Specificity, sensitivity
- Receptor binding
- Plasma protein binding

ESA

European Society for Autoradiography

www.autoradiography.eu

5th European Meeting. Uppsala 2004 (Click thumbnail to View)

Uppsala

Uppsala

Uppsala

ARG lecture

First autoradiography

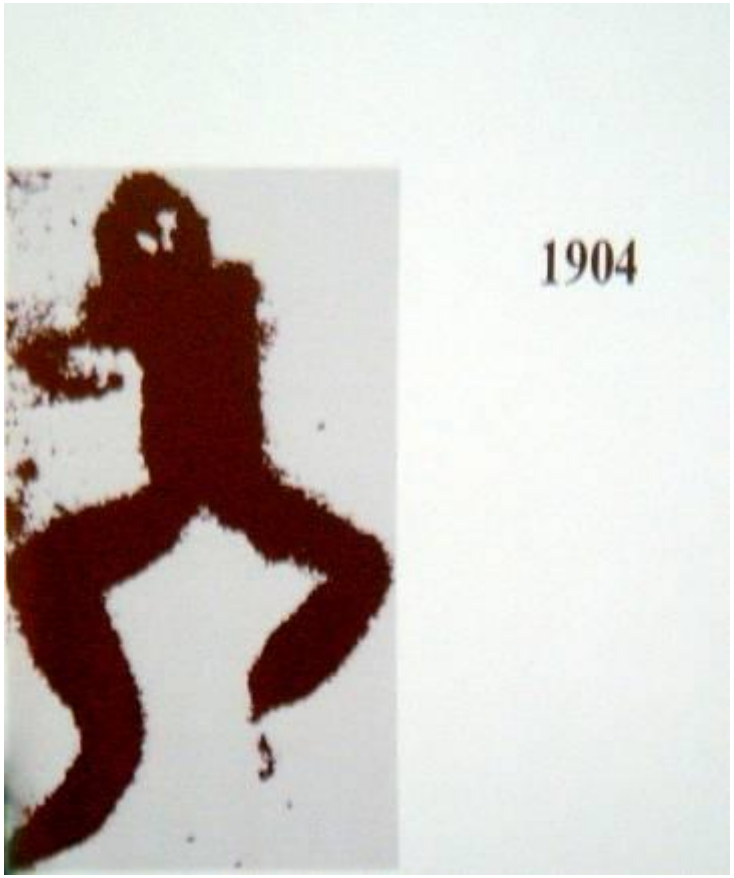

Ullberg 1954

embedding in cotton/ice water

compressed CO_2

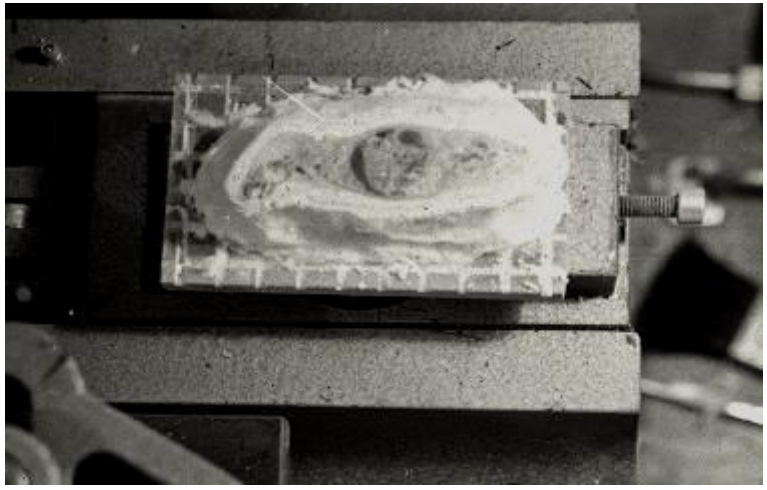

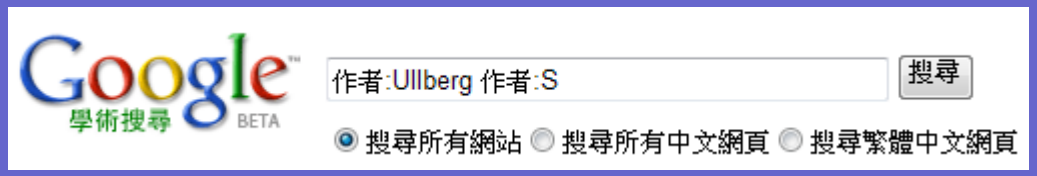

- Whole-body autoradiography in its present form has developed from Ullberg's original method (1954)
  - **[引言]** Studies on the distribution and fate of S35-labelled benzy] penicillin in the body **S Ullberg - 1954 - Esselte Aktiebolag** 被引用 299 次 - 相關文章 - 網頁搜尋
  - **[引言]** The technique of whole body autoradiography. Cryosectioning of large specimens **S Ullberg - Science Tools, 1977** 被引用 188 次 - 相關文章 - 網頁搜尋

Autoradiography

Bright 8250 Large surfaces Cryostat

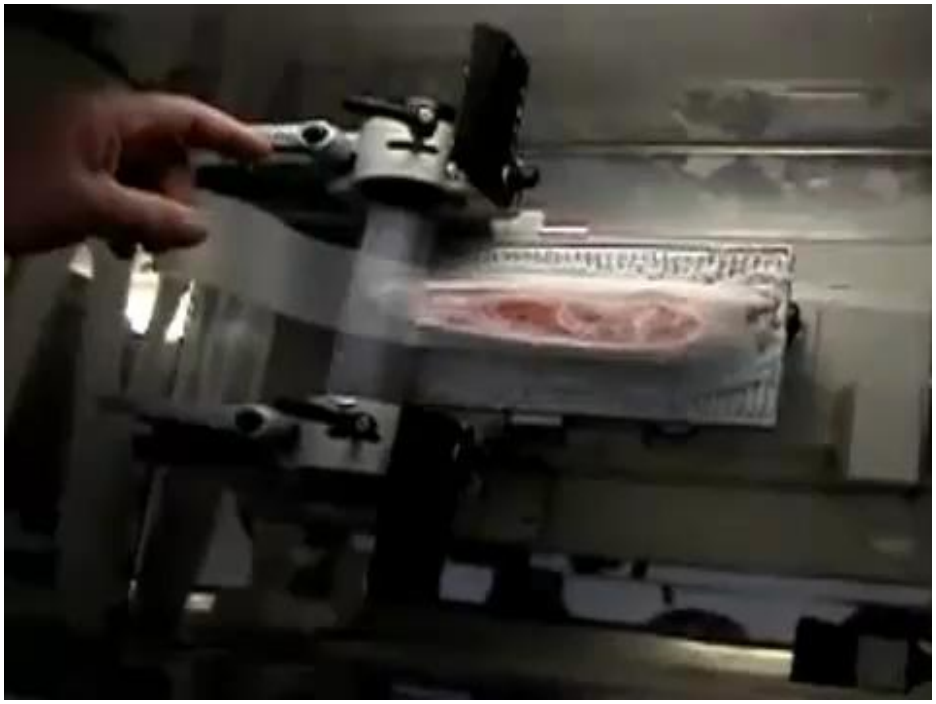

Macroautoradiographic

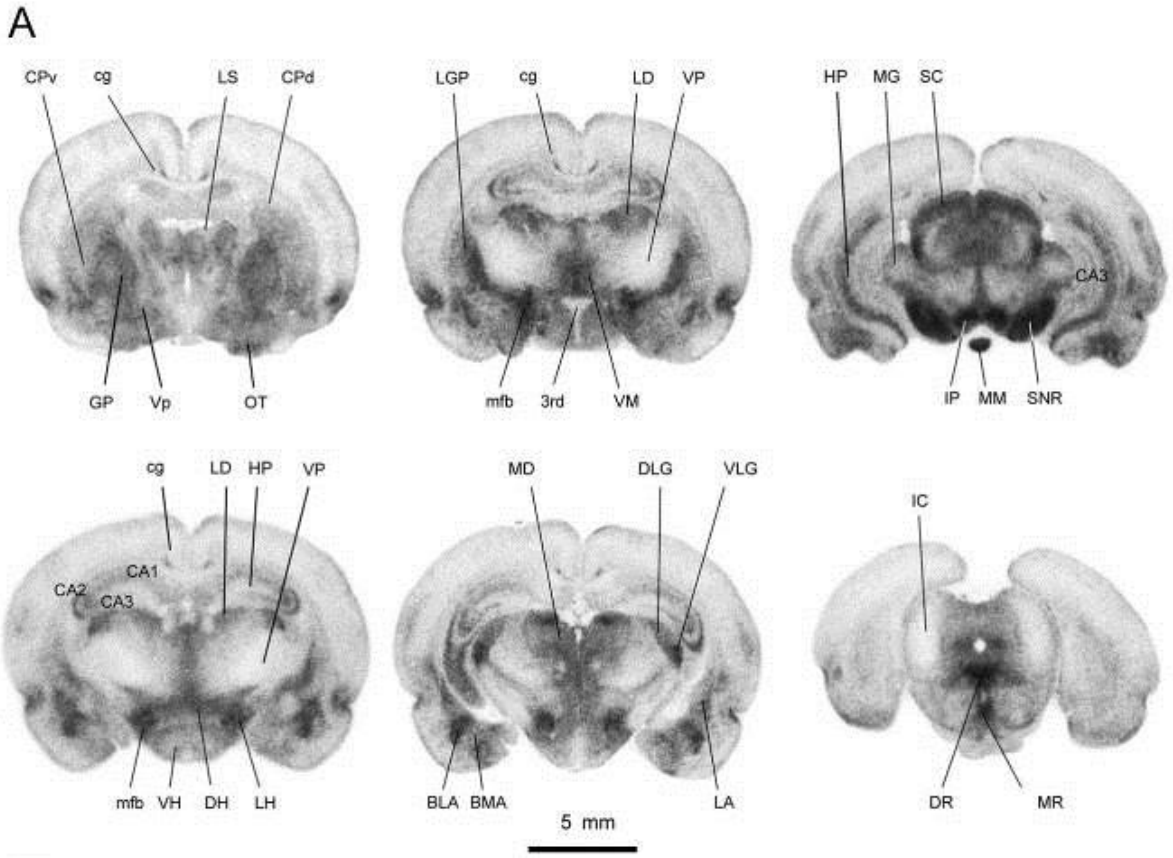

I-123 ADAM biodistribution (autoradiography)

Macroautoradiographic

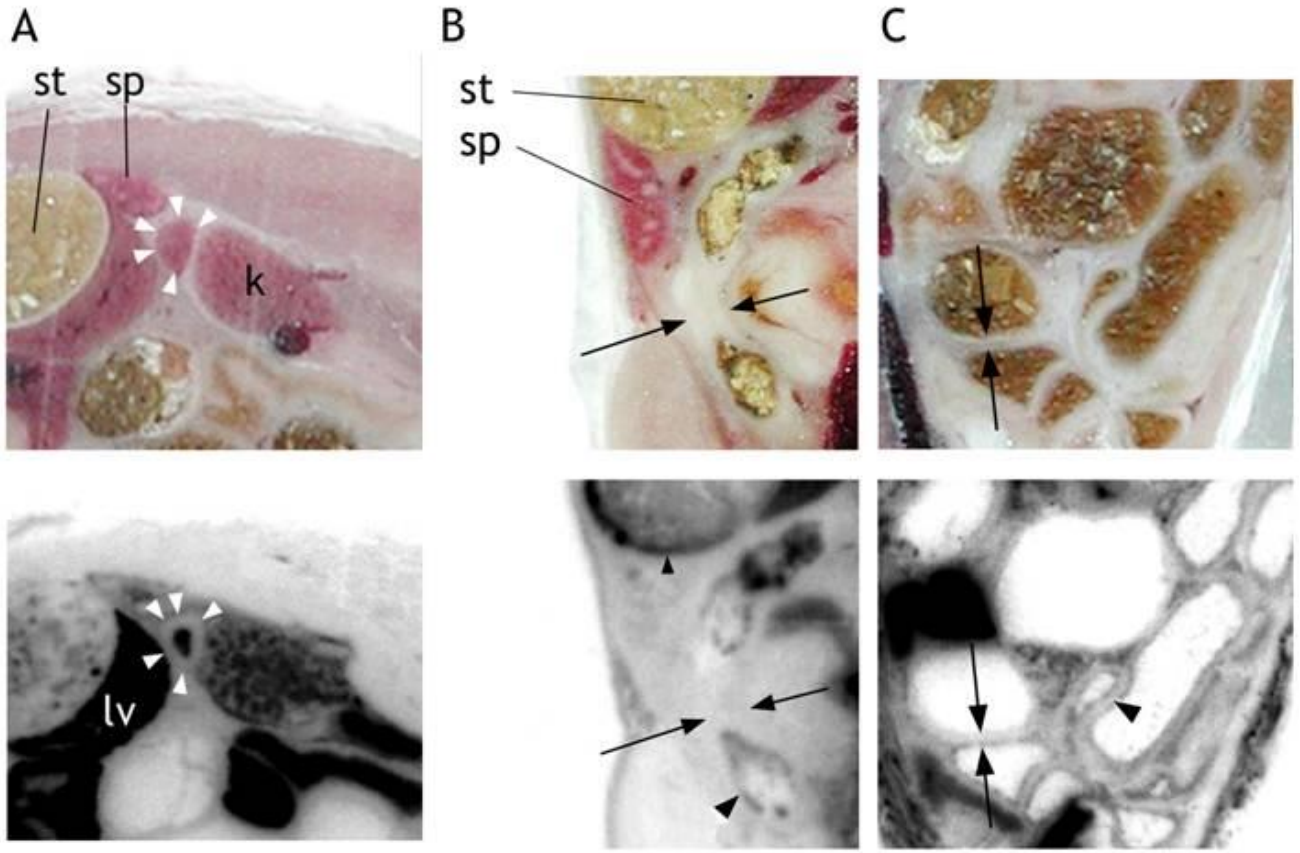

I-123 ADAM biodistribution (autoradiography)

Light microscopic autoradiograms

- **Combined thaw-mount autoradiography with immunohistochemistry of rat anterior pituitary**
- **i.v. injection of *^{3}H-1,25(OH)$_2$ vitamin D_3* stained by immunoperoxidase method with *antiserum to bovine beta-TSH*.**
- **Note the nuclear concentration of radioactivity in certain cells stained for TSH.**

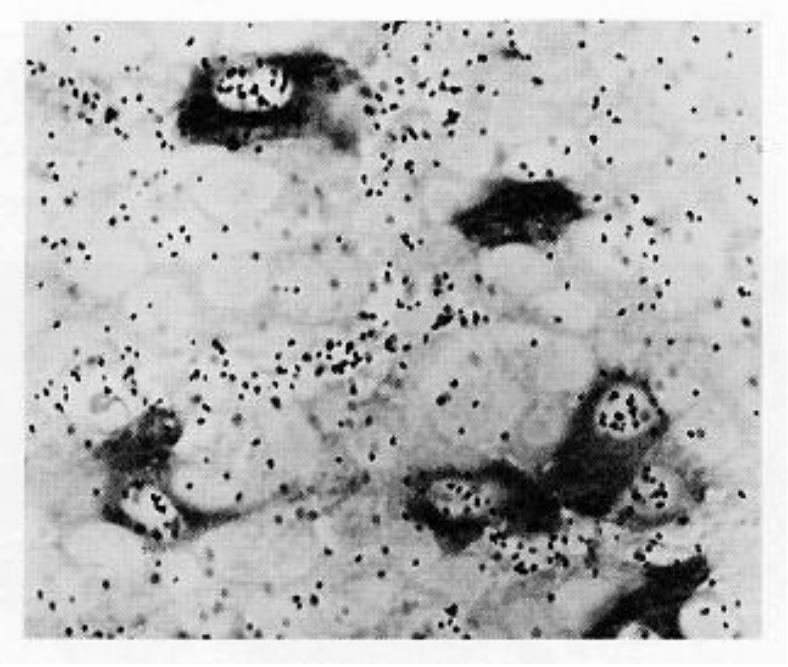

From Glenn, H. J. and Colombetti, L. G., Eds. Biologic Applications of Radiotracers. CRC Press, Inc., Boca Raton, Fl, 1982: 105. Previously from Sar, M., Stumpf, W. E. and DeLuca, H. F., Cell Tissue Res., 1980

4.Quantification for Biod.

- **Phosphor screen processed**
- **Calibration line constructed**
- **Tissue concentrations quantified**
- **Data processed ….**
- **Calculation for %ID**

Tissue measurement

- **Tissue dissection and counting**

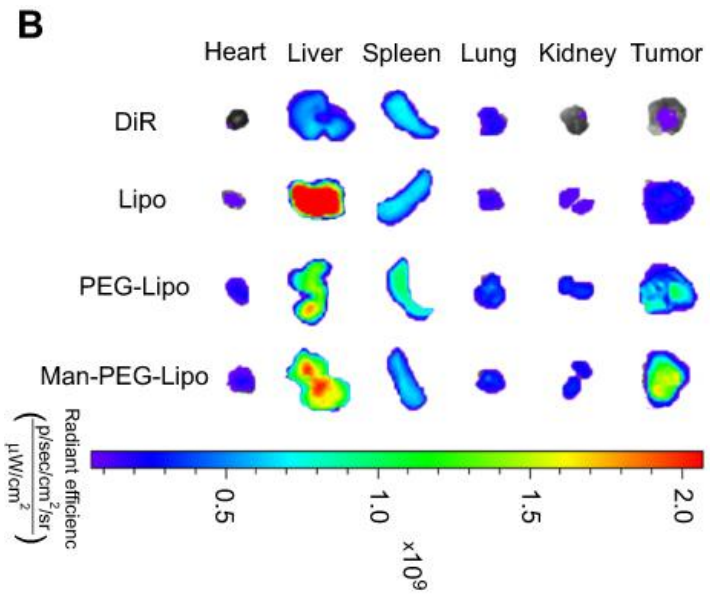

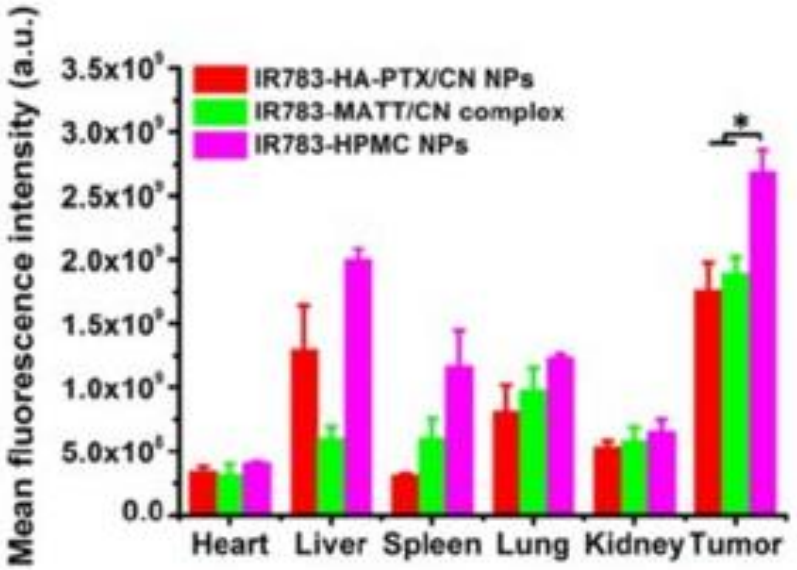

Normal tissue biod.

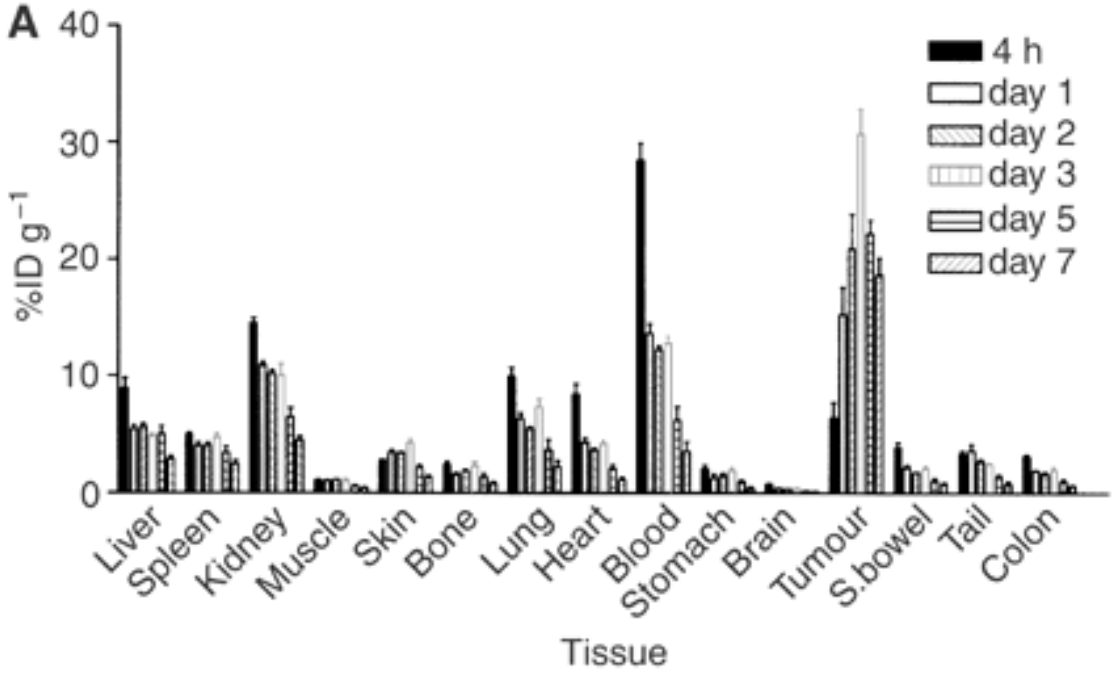

Normal tissue biodistribution of radiolabelled ch806 over 7 days in BALB/c nude mice bearing tumour xenografts (*n*=5). Results of the biodistribution of (**A**) 111In-CHX-A''-DTPA-ch806

Quantitative autoradiography

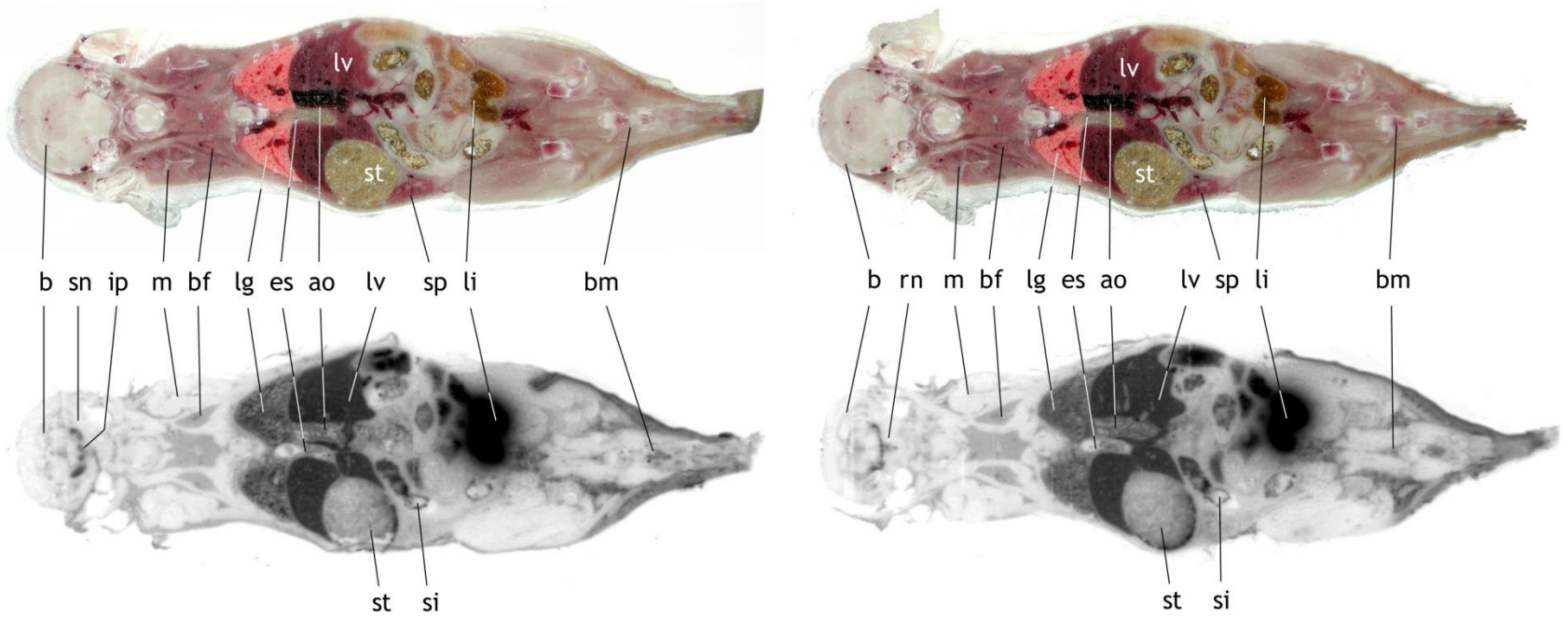

I-123 ADAM biodistribution (autoradiography)

IP scanning

- **Autoradiography IP scanning**

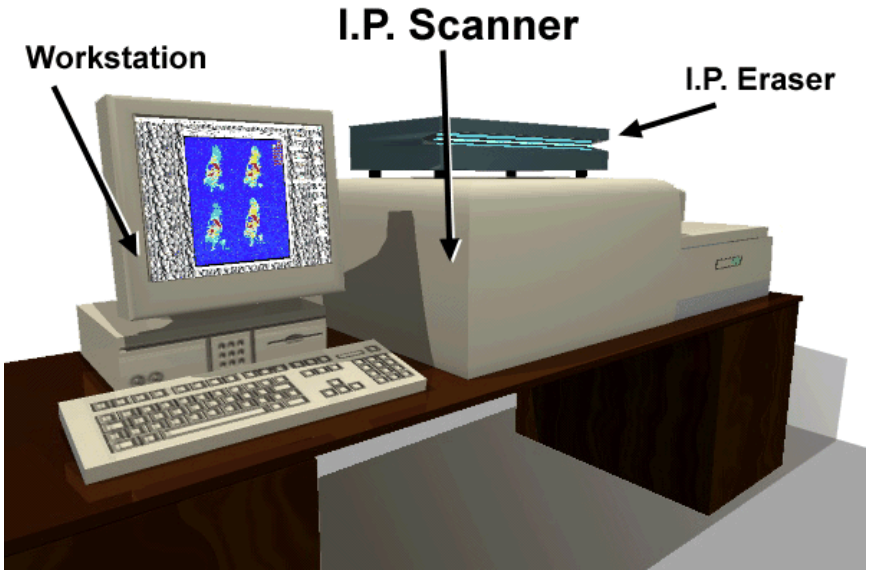

The Imaging Plate Scanner is a large device designed to capture and translate the radiation captured by the plate into a recognizable image.

IP scanning

- **The Imaging Plate composed of**
  - **a thin protective layer.**
  - **a photostimulable phosphor**
  - **flexible plastic support**

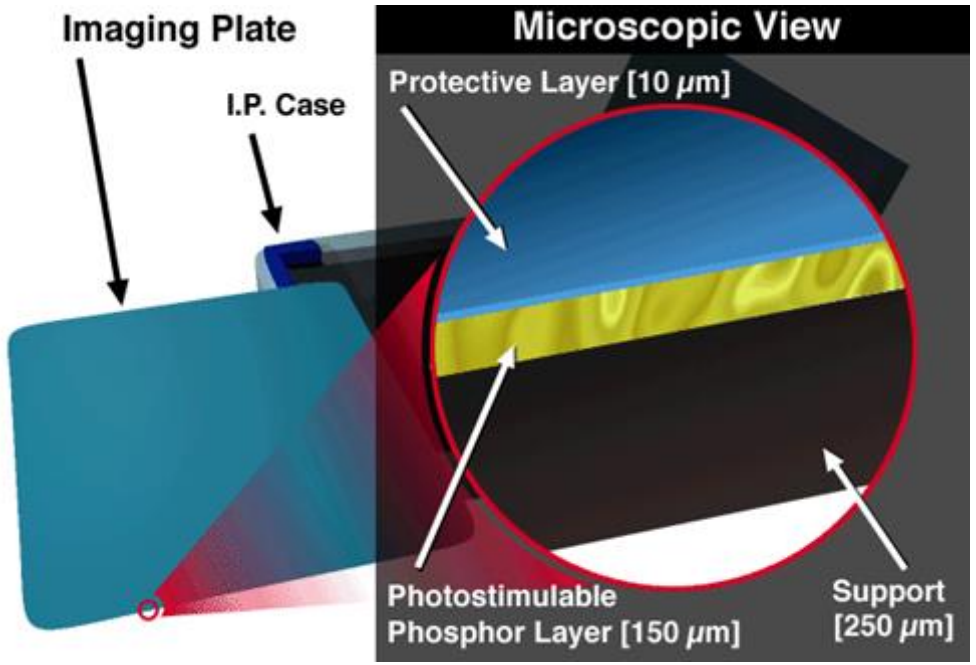

The phosphor is barium fluorobromide containing a trace amount of bivalent europium as a lumionescence center, BaFGBr:Eu2+.

IP scanning

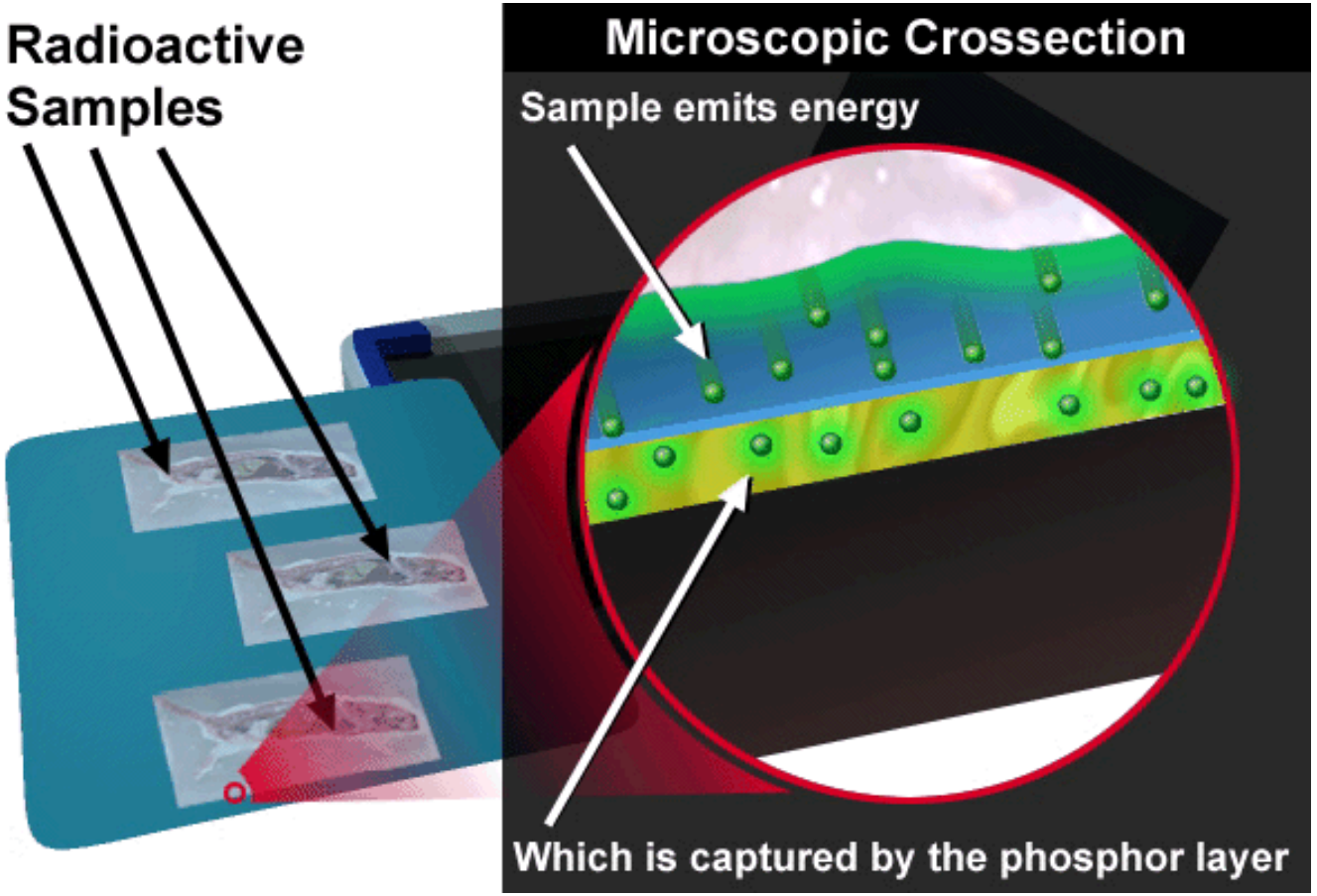
Radioactive
Samples
Microscopic Crossection
Sample emits energy
Which is captured by the phosphor layer

Exposures

Radionuclide	Exposure efficiency	Mean electron energy (keV) *	Half-life
^{14}C	1.0	54	5370 years
^{99m}Tc	2.3	120	6.0 hours
^{123}I	2.6	127	13.0 hours
^{131}I	2.9	200	8.0 days
^{18}F	3.1	250	1.8 hours
^{68}Ga	3.2	760	1.1 hours
^{124}I	3.1	850	4.2 days
^{3}H	**	6	12.5 years
^{11}C	unavailable	380	20.4 minutes

IP scanning

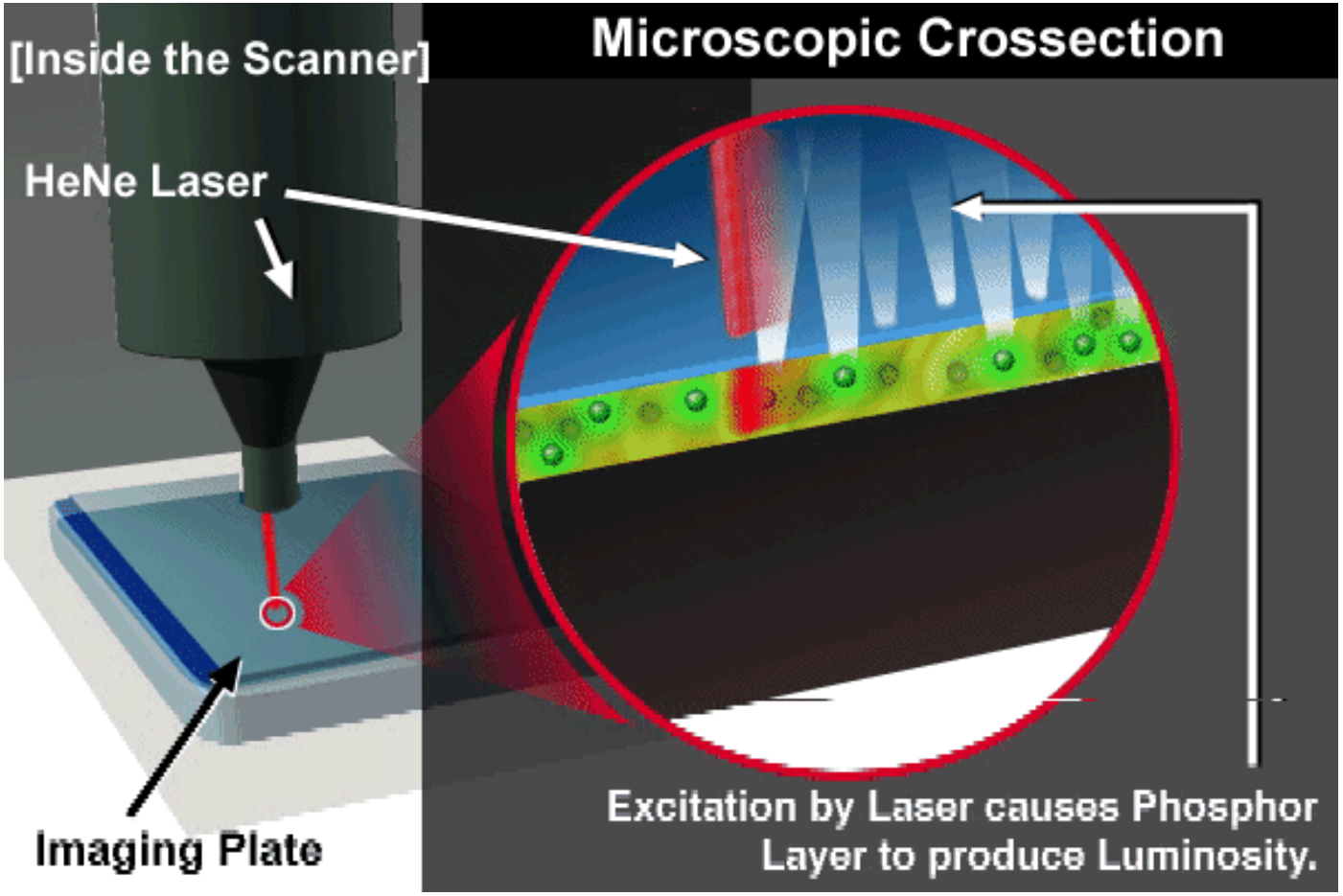
[Inside the Scanner]
Microscopic Crossection
HeNe Laser
Imaging Plate
Excitation by Laser causes Phosphor
Layer to produce Luminosity.

The blood quantification

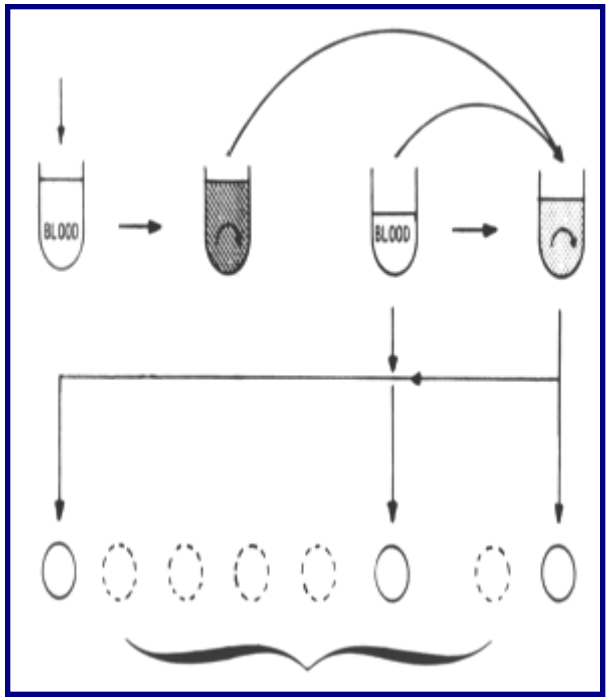

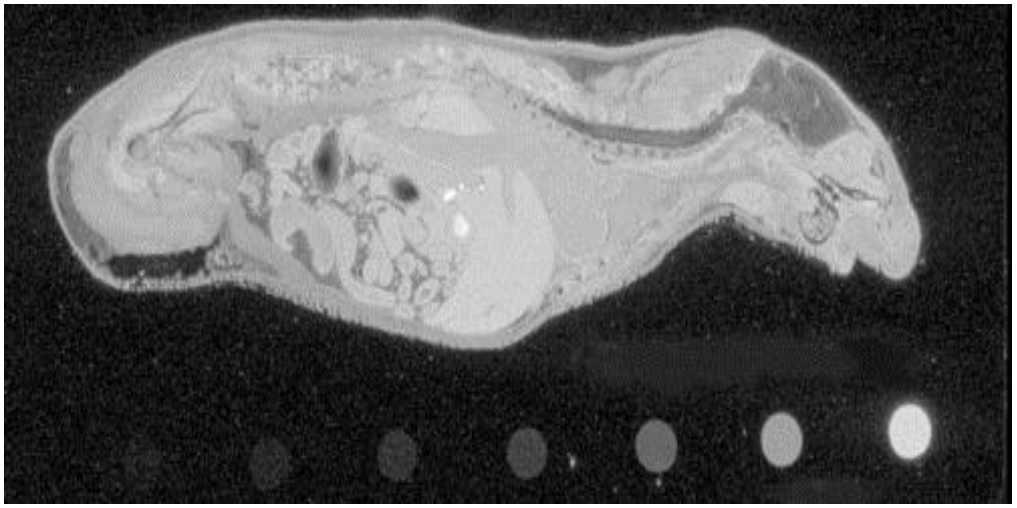

Quantification

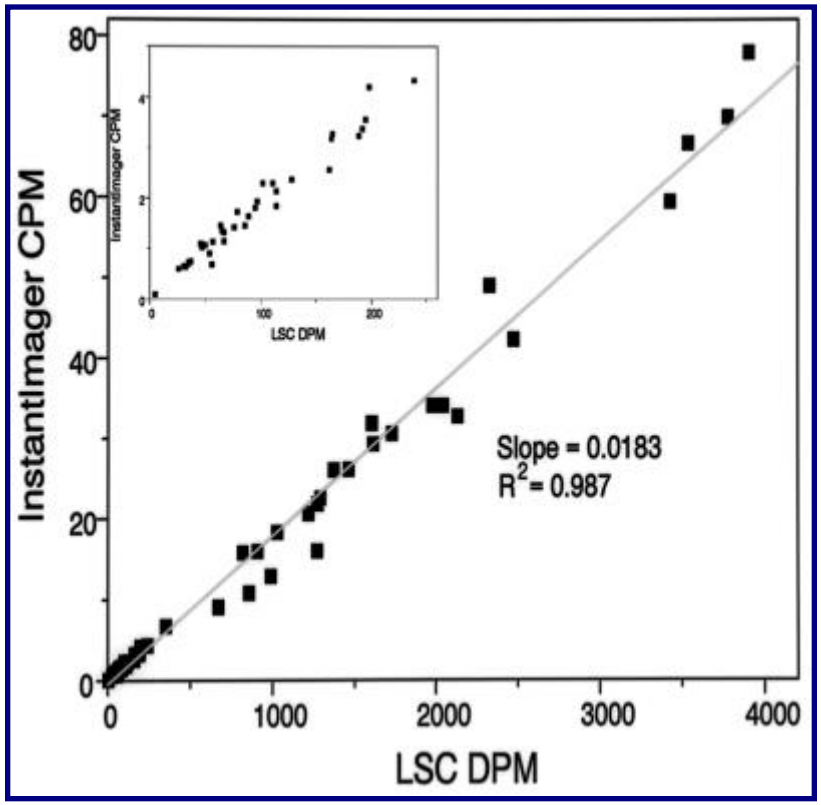

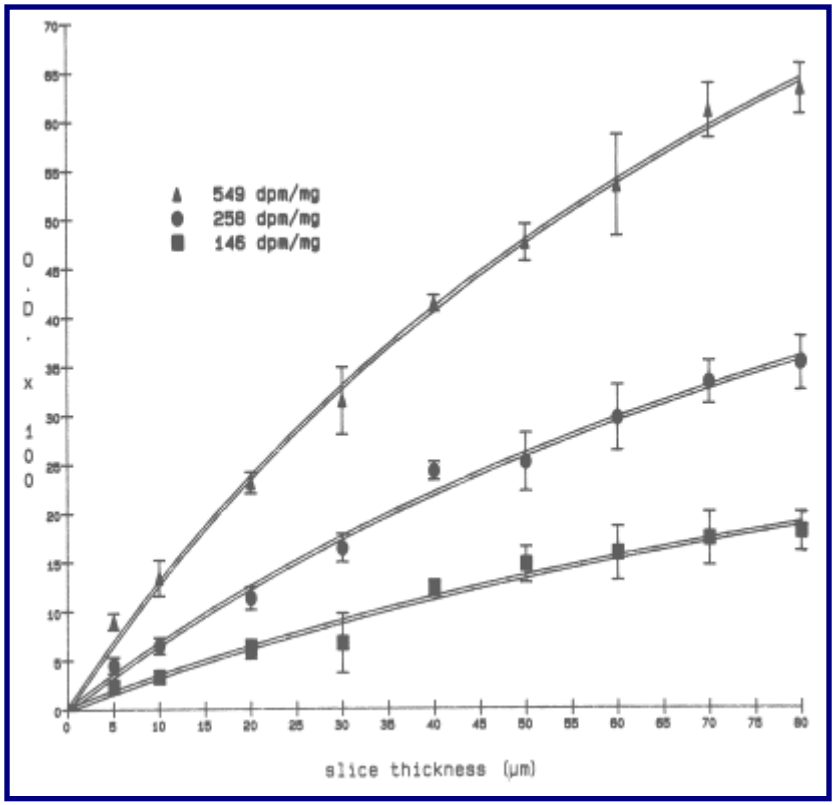

DPM, CPM correlation, slides thickness

Resolution

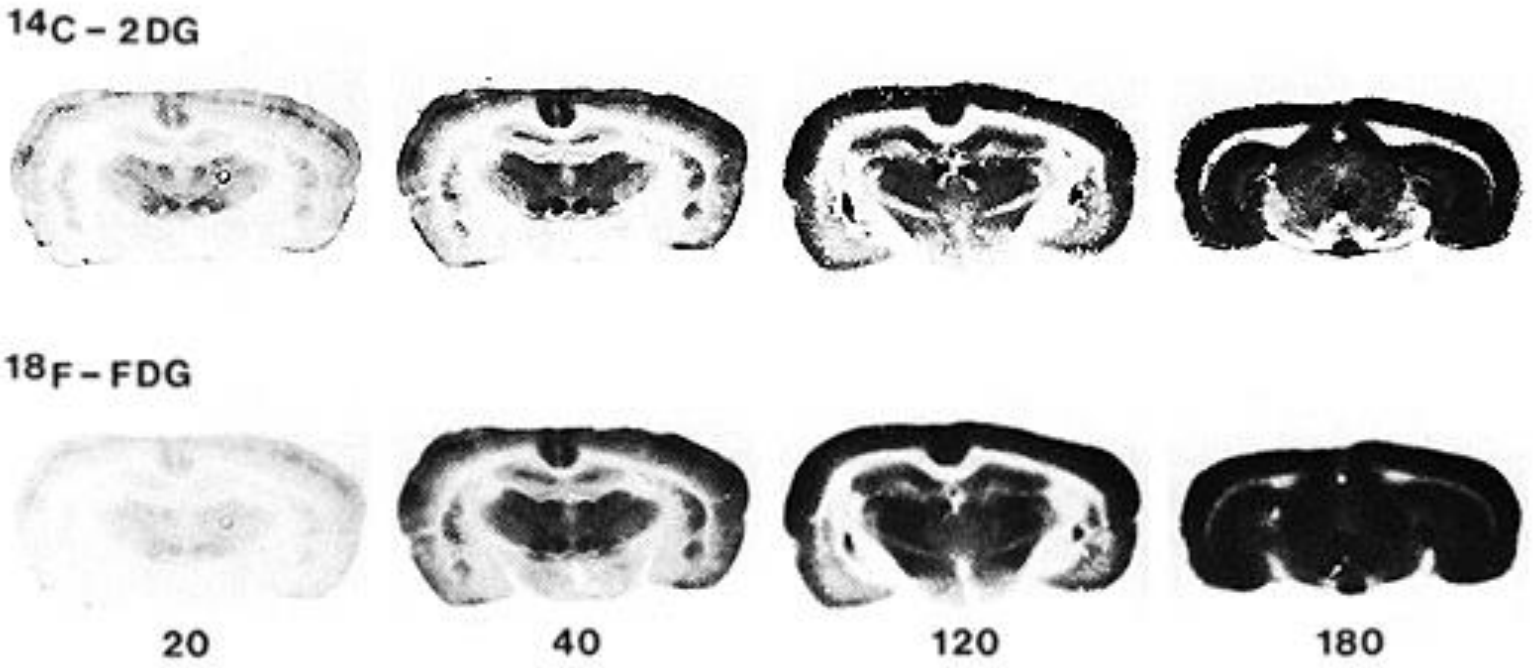

Resolution is reduced for the higher-energy emitter and deminishes as tissue thickness increases.

The available software

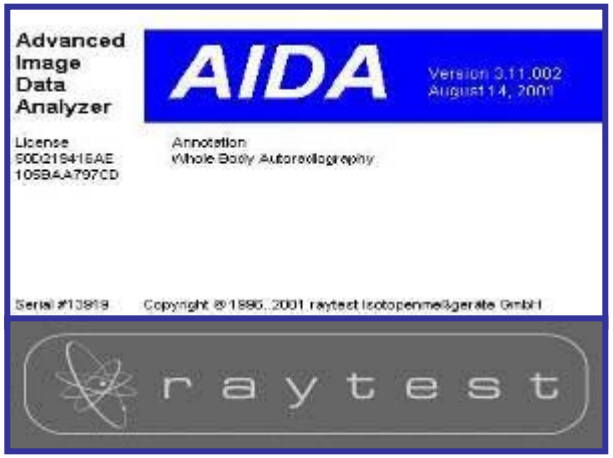

	AIDA	MCID	Seescan 2
Target use	Multifunctional by module	Multifunctional	Dedicated QWBA
User friendliness/ Complexity	Easy to use for QWBA	Easy to use for QWBA	More complex due to GLP features
Operating area	Stand alone	Stand alone	Stand alone or LIMS linked
GLP/CFR compliance	Claimed	No	Claimed
Protocol	No	No	Yes
Data Export	Yes	Yes	Yes
Tabulation	In external software (eg Excel)	In external software (eg Excel)	Some via DMS more through LIMS link
Area of use	Discovery and GLP/Regulatory	Discovery	Discovery and GLP/Regulatory
Image output	Yes	Yes	Yes
Manufacturer Support	Yes	Yes	Yes

DMS - Document Management System

Electron microscopic autoradiography

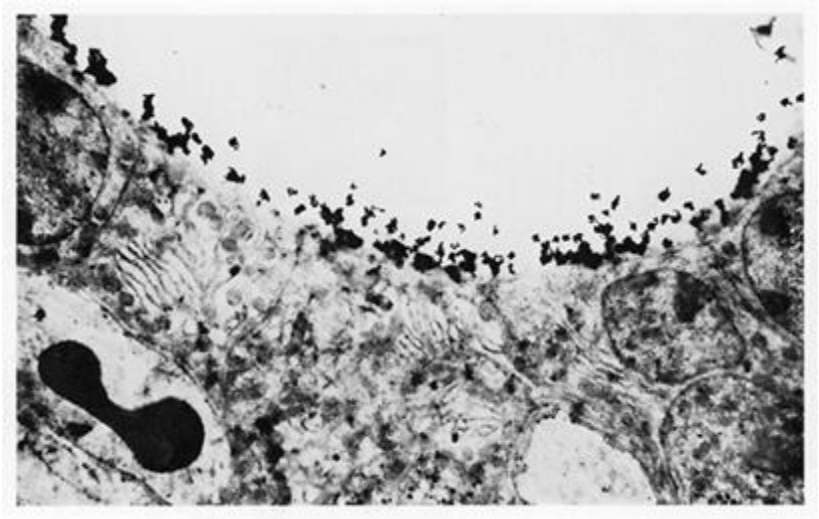

From Glenn, H. J. and Colombetti, L. G., Eds. Biologic Applications of Radiotracers. CRC Press, Inc., Boca Raton, Fl, 1982: 106. Previously from Dohlman, G. F., Maunsbach, A. B., Hammarstrom, L., and Appelgren, L. E., J. Ultrastruct. Res., 10, 293, 1964

- **Electron microscopic autoradiogram of a mouse thyroid, showing the distribution of ^{125}I, 1 hr after injection.**
- **The radioactivity is confined to the colloid, just outside the thyroid cells, which indicates *formation of thyroid hormone at the colloid side of the cell membrane*.**

Electron microscopic autoradiography

- **An electron microscopic autoradiogram which shows ^{125}I-labeled alphabungarotoxin bound to the acetylcholine receptor of a neuromuscular junction.**
- **The silver grains are localized close to the axon at the tops of the post-junctional folded membrane.**

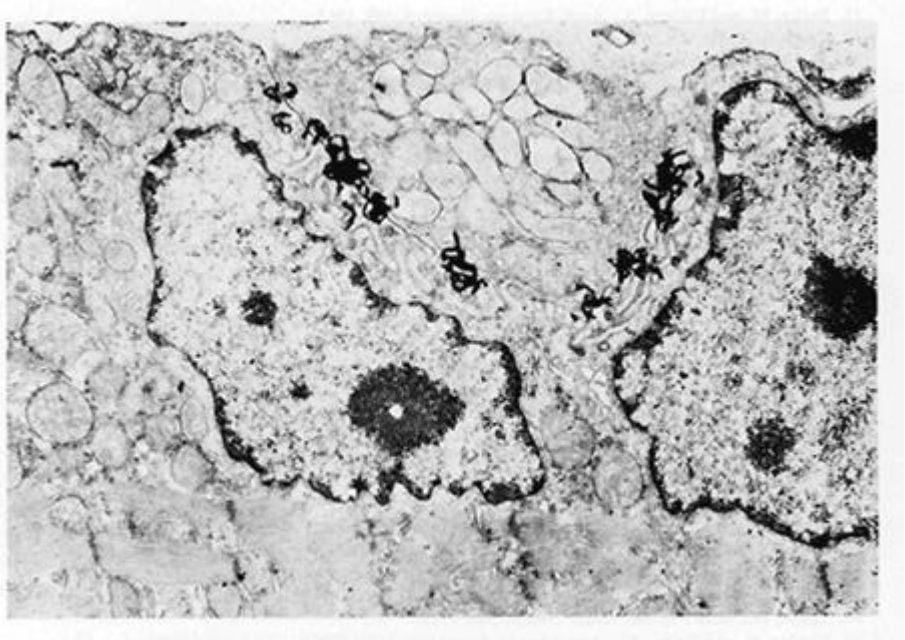

From Glenn, H. J. and Colombetti, L. G., Eds. Biologic Applications of Radiotracers. CRC Press, Inc., Boca Raton, Fl, 1982: 107. Previously from Fertuch, H. C. and Salpeter, M. M., J. Cell. Biol., 69, 144, 1976

5.Animal study

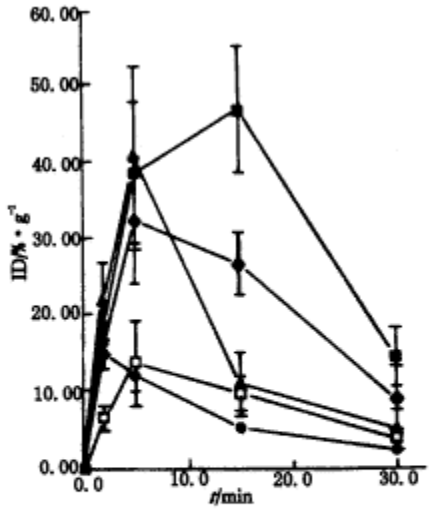

图5 pH=4时$^{99}Tc^{m}$-BPHA的生物分布

Fig.5 Biodistribution of $^{99}Tc^{m}$-BPHA formed at pH=4

■——肾；◆——肝；▲——肺；□——脾；●——血

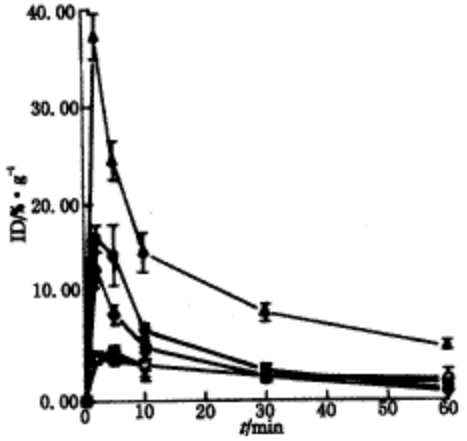

图6 pH=7时$^{99}Tc^{m}$-BPHA的生物分布

Fig.6 Biodistribution of $^{99}Tc^{m}$-BPHA formed at pH=7

▲——肾；●——血；◆——肺；□——肝；○——脾

Input function from blood

- Heparinized micro-hematocrit tubes, microcentrifuge tubes (1.5 μ L) and reverse-phase micro TLC plates
- Radioactivity in blood samples and extracts are determined as counts per minute [CPM] using a WIZARD2 automatic gamma counter.
- Blood samples are collected by tail artery puncture at 5, 15, 30, 45 and 75 min post injection
- The blood samples are radioassayed in a gamma well counter to determine radioactivity in the ‘whole blood’, then in plasma, cellular and protein fractions.

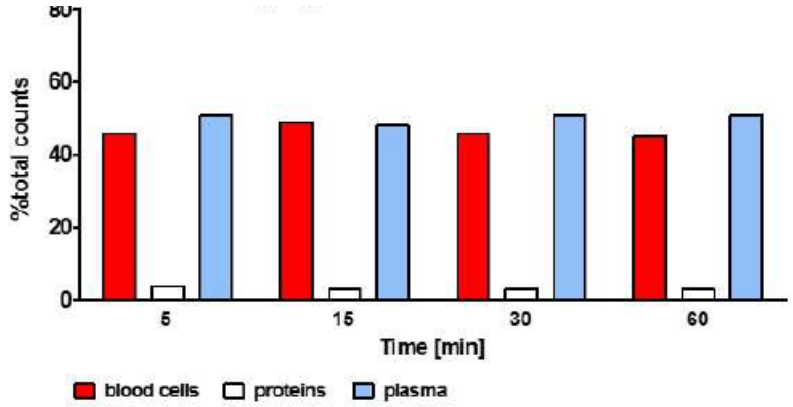

Input function from image

- image-derived input function.

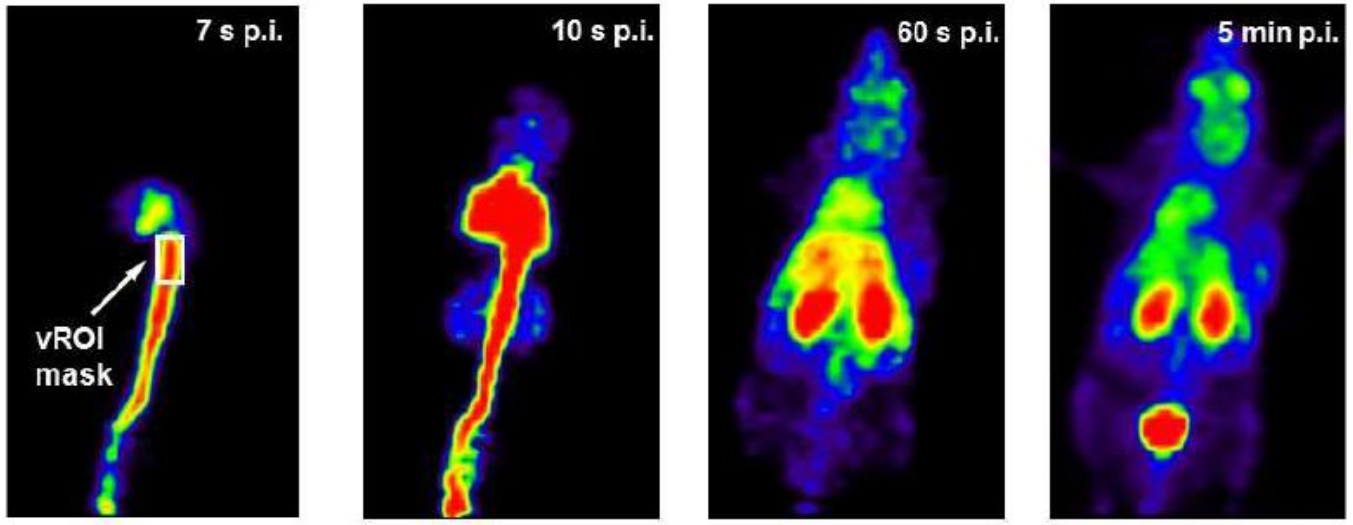

- Common vROI for image-derived input function are inferior vena cava or heart.
- Spillover from myocardial uptake, partial volume effects and heart motion all contribute to the uncertainty

Time activity curve

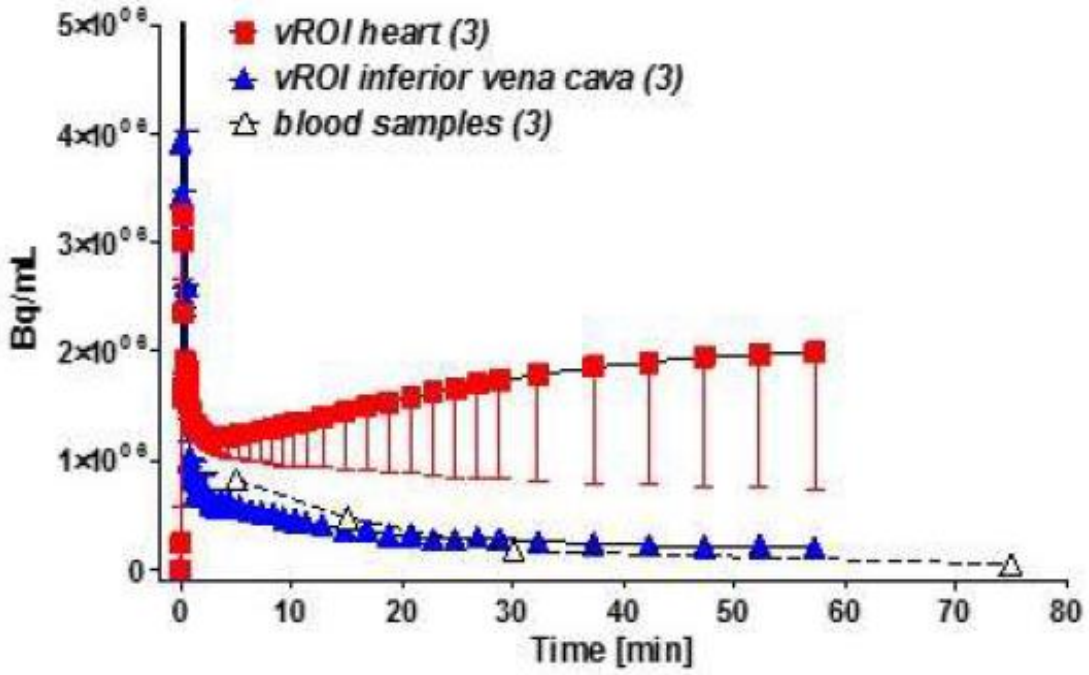

- PET image Time-activity curves (TACs) for vROI over the heart and inferior vena cava in comparison to data from direct blood samples after injection.

Metabolite correction

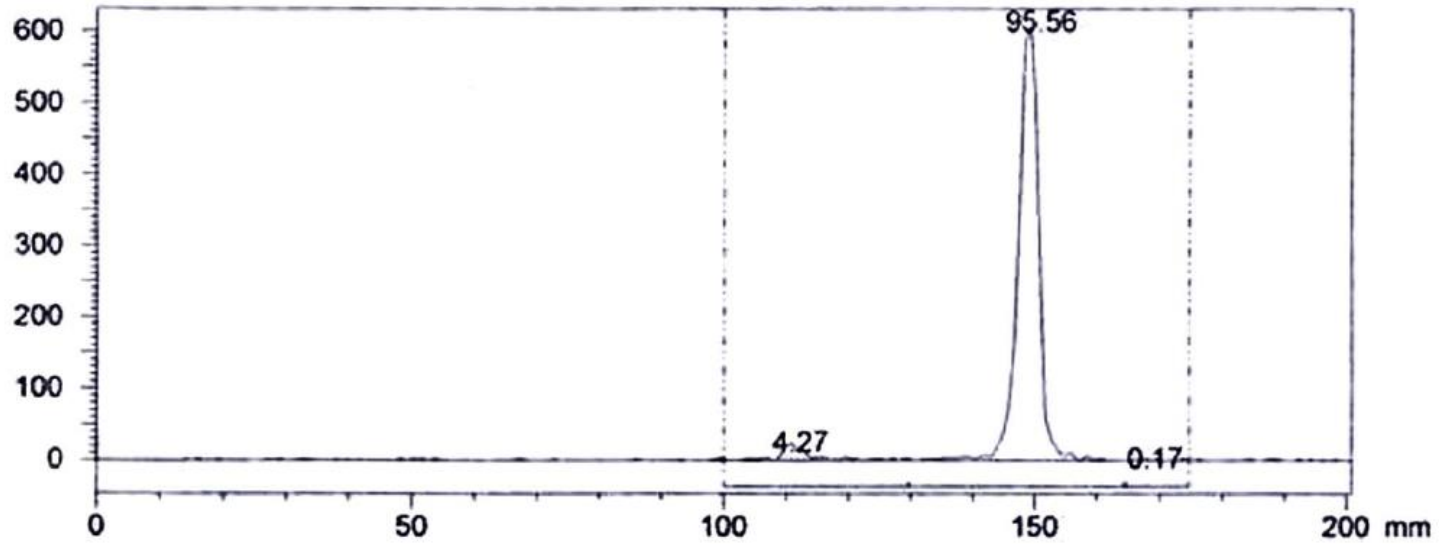

- A representative radio-microTLC elution profile of the methanolic extract of arterial tail vein whole blood. The peak at 150 mm co-chromatographed with authentic X and accounted for 96 % of the radioactivity on the plate.
- Metabolite correction: PET data reflect total counts from all radioactivity present in the defined vROI (i.e., not drug only, but also all radioactive metabolites).

Modeling estimate

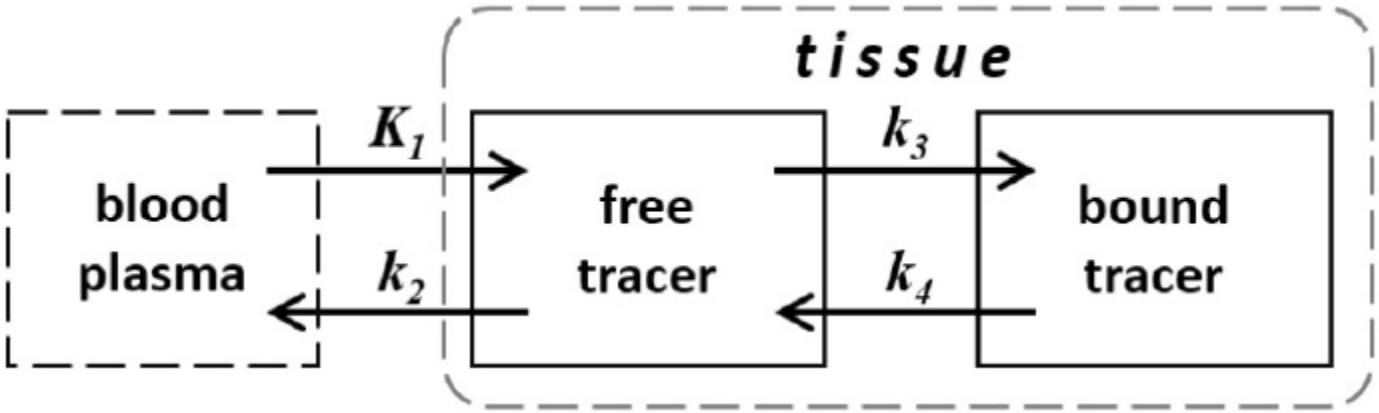

The two-compartment kinetic model: the first compartment represents free tracer inside a cell (cell membrane transport described by K1 and k2); the second compartment represents modified tracer molecules; these processes and their reverse are described by the rate constants k3 and k4, respectively.

Modeling fitting

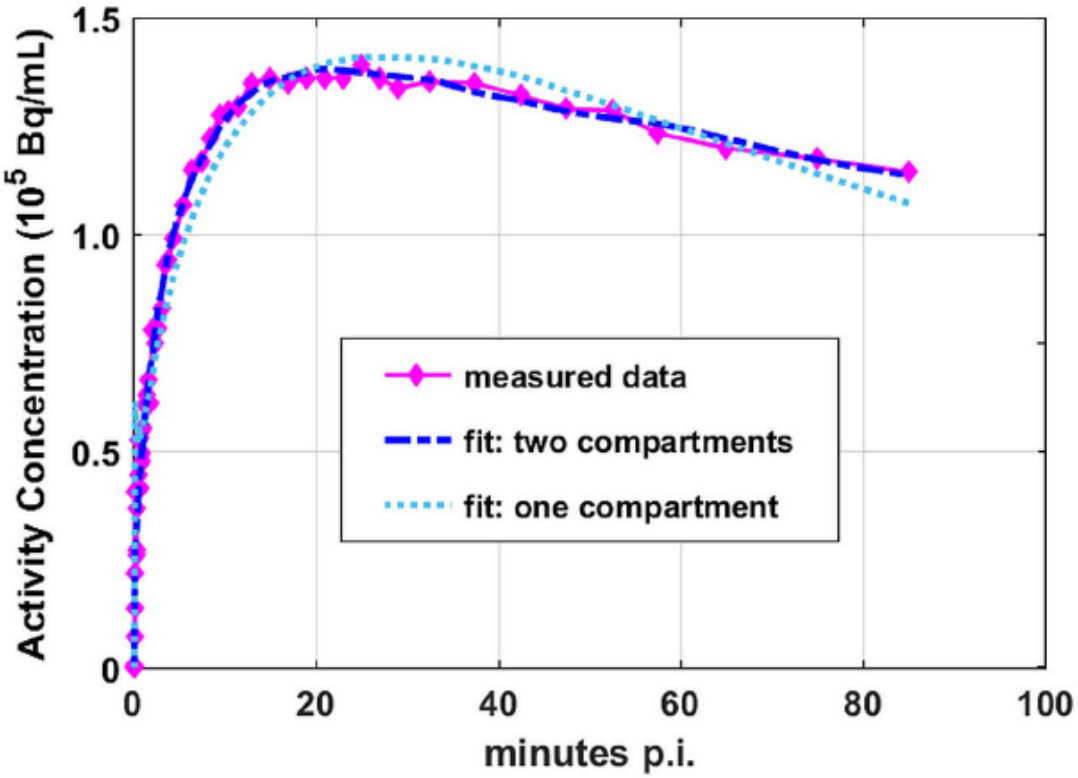

Measured PET data points for radiotracer fitted with a two-compartment model (dashed) and one-compartment model (dotted)

6.Human study

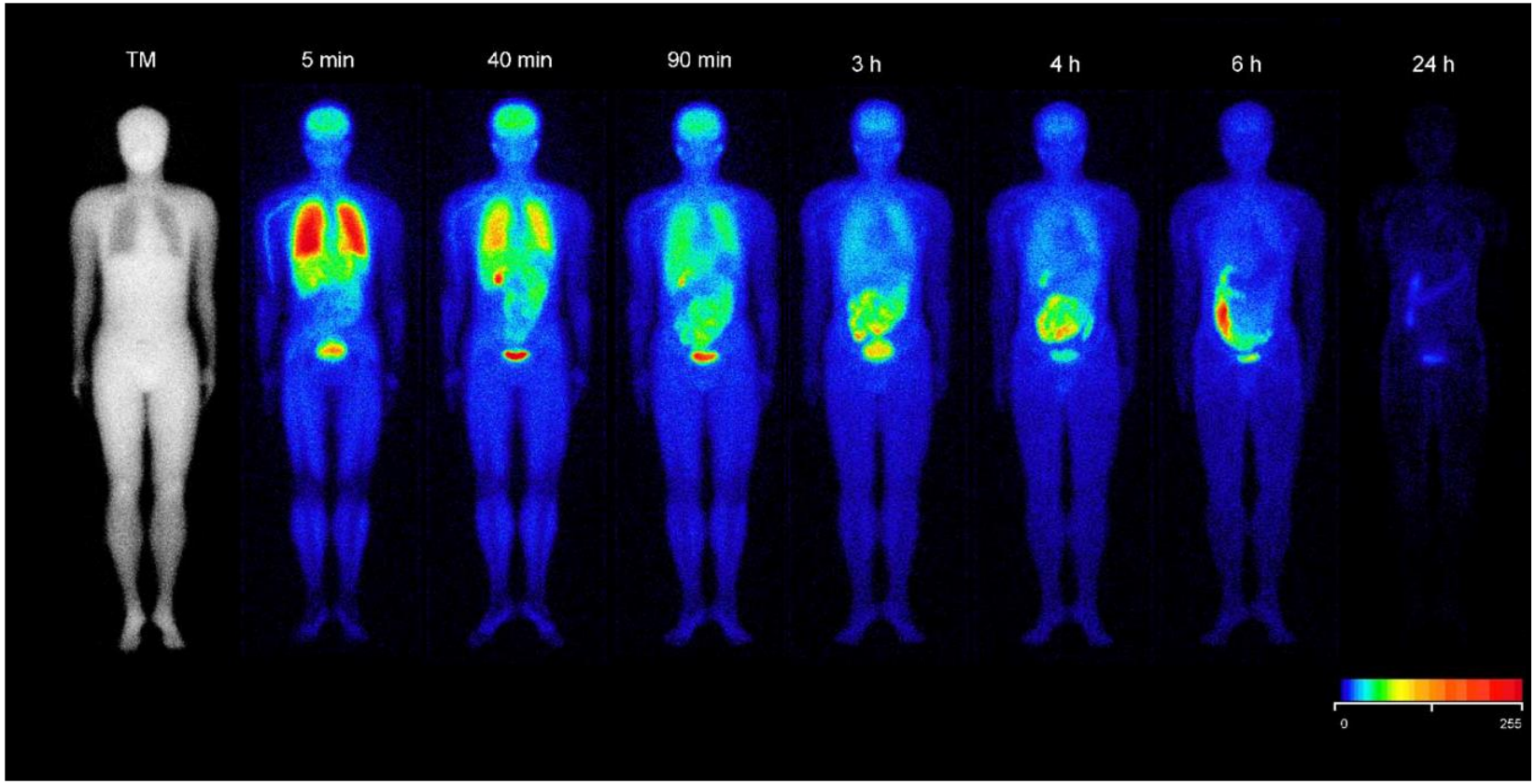

如何計算？（SPECT定量）

- **ROI (VOI)**
- **Geometric meam**
- **Attenuation correction**
- **Decay correction**
- **%ID calculation**

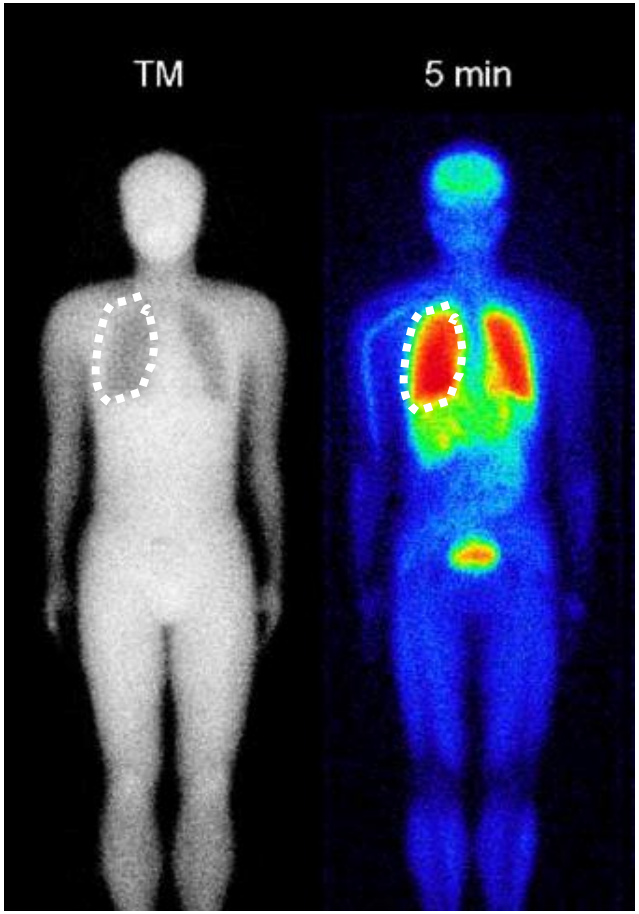

PET QC

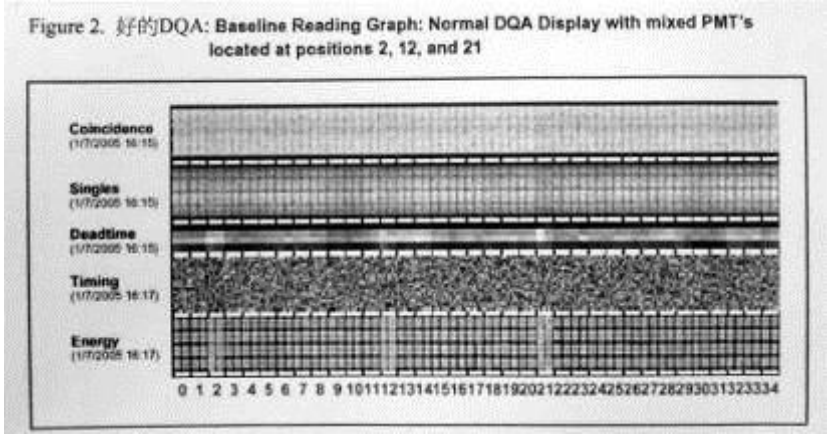
Figure 2. 好的DQA: Baseline Reading Graph: Normal DQA Display with mixed PMT's located at positions 2, 12, and 21
Coincidence
Singles
Deadtime
Timing
Energy
0 1 2 3 4 5 6 7 8 9 10 11 12 13 14 15 16 17 18 19 20 21 22 23 24 25 26 27 28 29 30 31 32 33 34

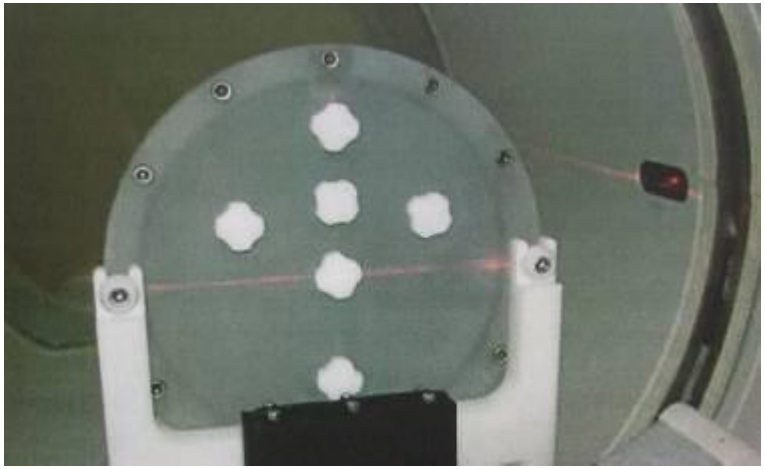

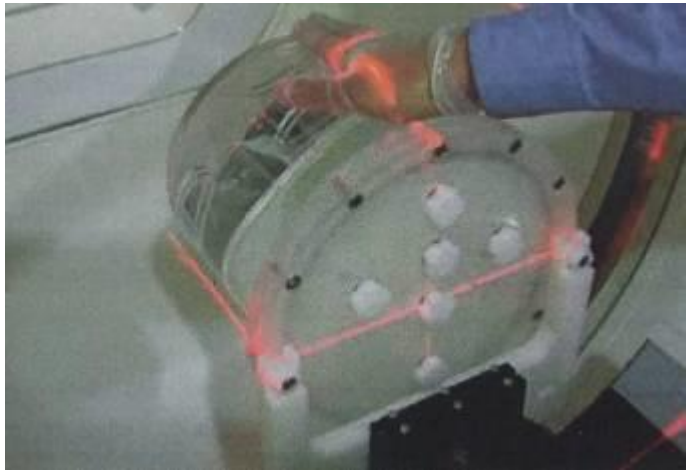

Phantom study

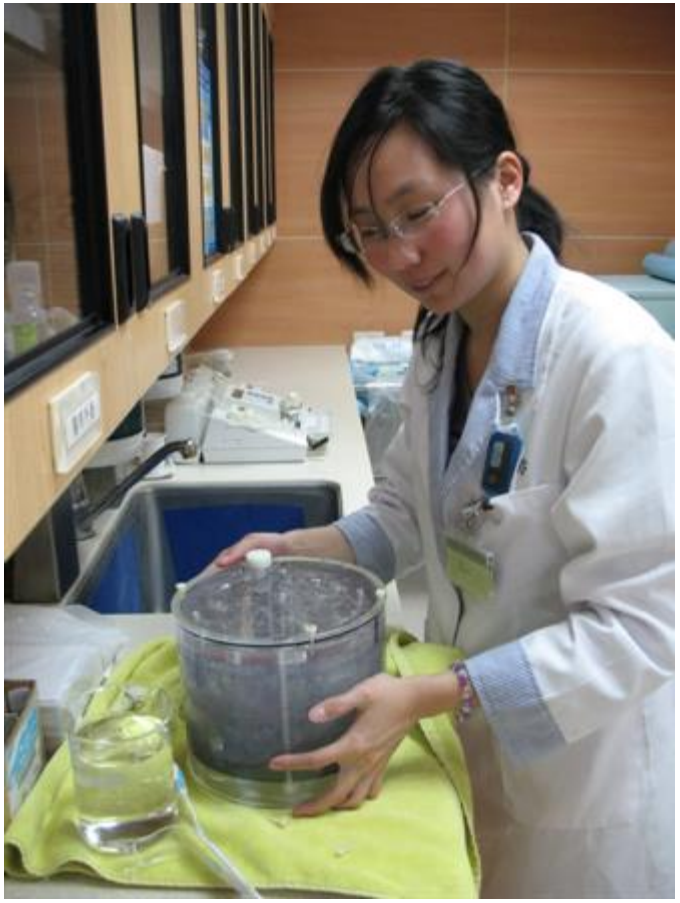

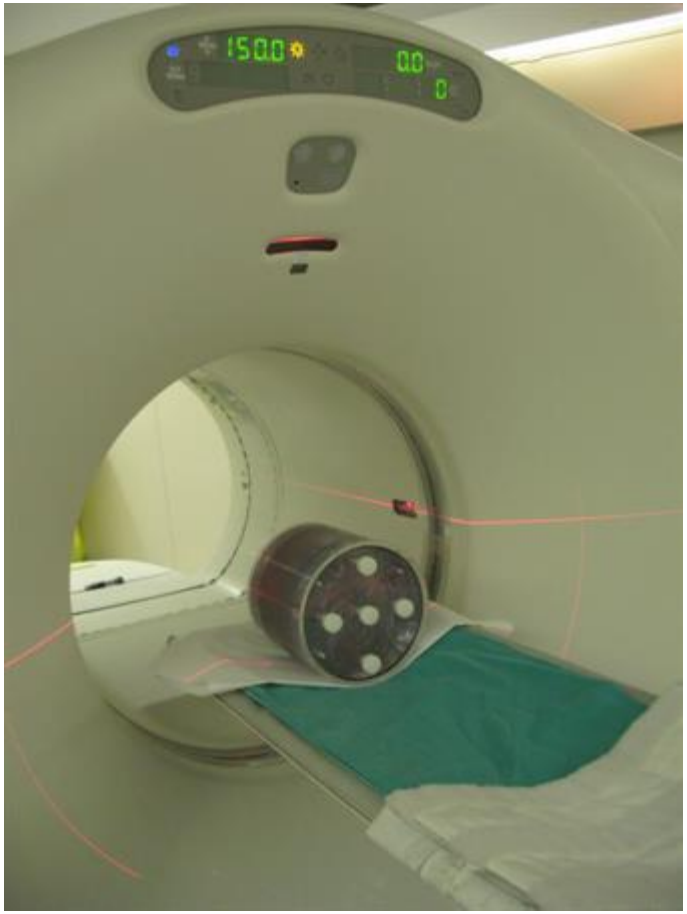

Image quality

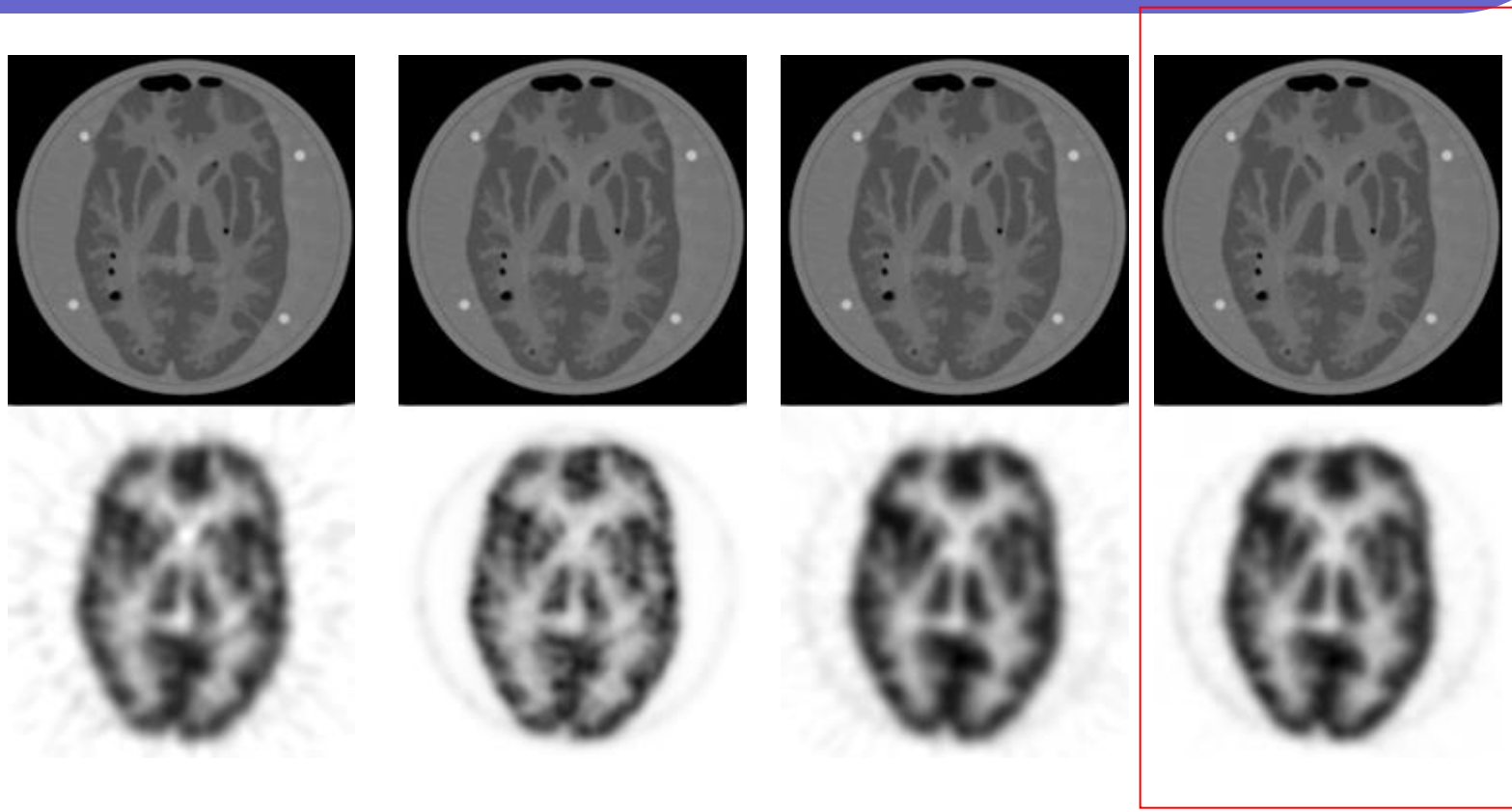

2D FBP

2D OSEM
4 iteration, 15 subsets

3D FBP

3D OSEM
4 iteration, 16 subsets

如何計算？（PET定量）

PET Quantifiation

Percentage injected dose (%ID)

$$\text{SUV} = \frac{\text{Decay corrected tissue activity (Bq/mL)}}{\text{Injected dose (Bq) / Body weight (g)}},$$

$$\%ID\ (t) = 100\% \times \overline{SUV}_{organ}(t) \times \frac{M_{organ}}{M_{wholebody}},$$

Whole body biod.

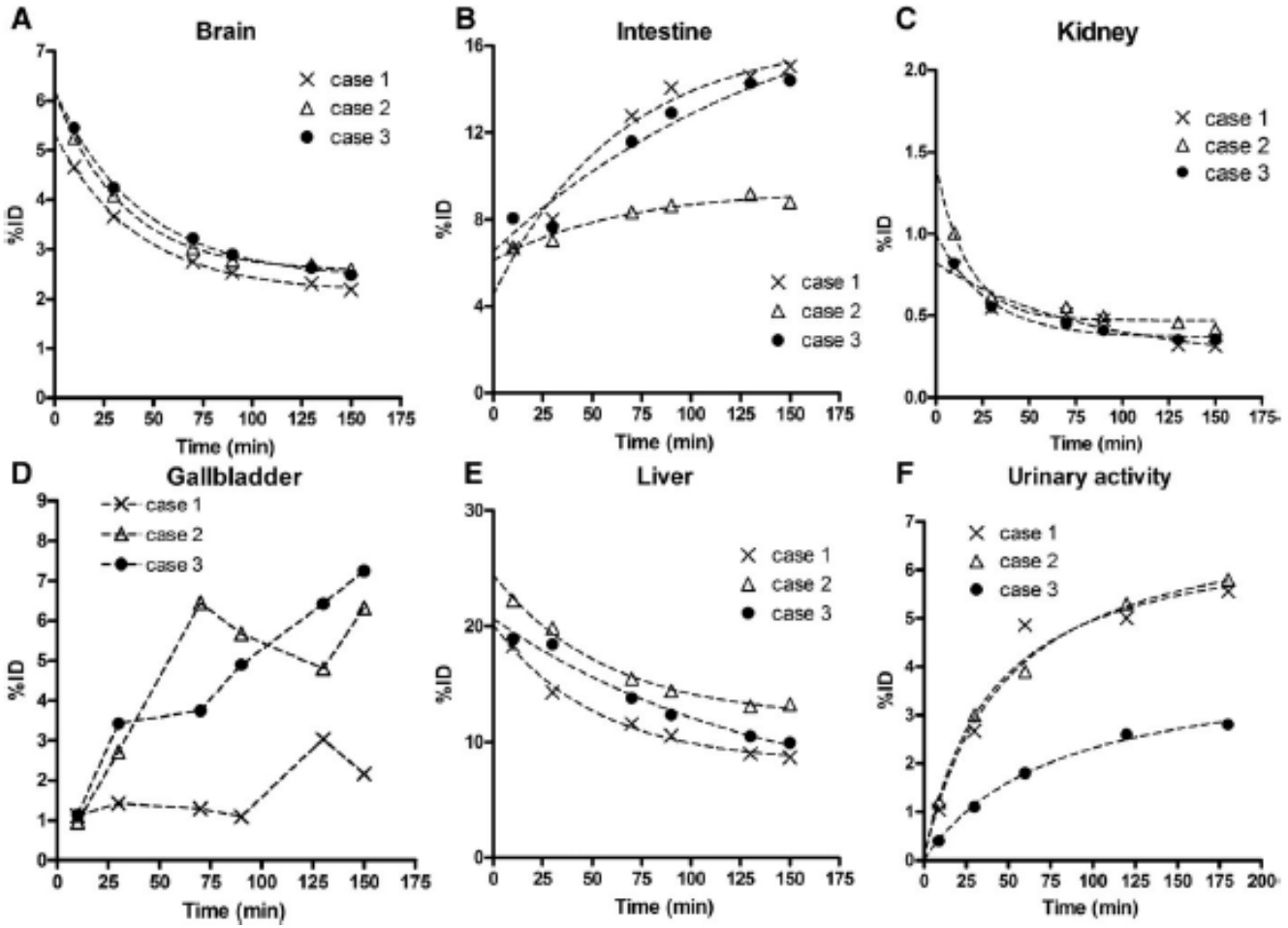

7. 新藥開發注意事項

- 瞭解新藥的代謝途徑，可能副作用，協助新藥開發
- 瞭解藥物對重要器官的累積輻射劑量
- 瞭解藥物的正常分佈以及異常分佈
- 瞭解可給予的最大劑量
- 瞭解治療劑量

Radiation dosimetry

[^{18}F]AV-45 radiation doses for a 73.7-kg adult phantom

Urine interval	2.4 h			4.8 h		
Subject No.	1	2	3	1	2	3
Adrenals	13.2	14.8	13.8	13.3	14.8	13.8
Brain	12.5	14.4	14.4	12.5	14.4	14.4
Breasts	7.4	7.6	7.37	7.4	7.6	7.4
Gallbladder wall	94.0	226.0	234.0	94.1	226.0	234.0
LLI wall	28.8	21.6	26.6	29.3	22.1	26.9
Small intestine	62.7	43.5	59.5	62.9	43.7	59.6
Stomach wall	17.1	15.5	14.8	17.2	15.5	14.8
ULI wall	70.1	48.9	67.2	70.2	49.1	67.3
Heart wall	14.8	16.3	15.8	14.8	16.3	15.8
Kidneys	15.3	17.9	16.5	15.4	18.0	16.5
Liver	36.8	52.6	43.8	36.8	52.7	43.8
Lungs	9.7	10.9	10.3	9.7	10.9	10.3
Muscle	9.9	9.8	9.7	10.0	9.9	9.8
Ovaries	19.4	16.3	18.1	19.9	16.8	18.4
Pancreas	14.3	16.1	15.5	14.3	16.1	15.5
Red marrow	19.7	20.6	15.5	19.8	20.7	15.6
Osteogenic cells	18.7	19.2	16.3	18.8	19.3	16.4
Skin	7.0	7.0	6.9	7.1	7.0	6.9
Spleen	10.6	10.5	10.5	10.6	10.5	10.5
Testes	8.7	8.4	8.2	9.1	8.8	8.4
Thymus	9.0	9.2	9.0	9.0	9.2	9.0
Thyroid	8.5	8.5	8.3	8.5	8.5	8.3
Urinary bladder wall	41.2	39.9	23.4	60.3	59.3	32.8
Uterus	18.0	15.8	16.4	19.2	17.0	17.0
Total body	11.8	12.0	11.7	11.9	12.1	11.8
Effective dose equivalent (μSv/MBq)	28.6	34.5	35.3	29.9	35.8	35.8
Effective dose (μSv/MBq)	20.0	18.2	18.2	21.2	19.3	18.7

Data are presented in μGy/MBq unless otherwise indicated. LLI, lower large intestine; ULI, upper large intestine.

Source and target organs

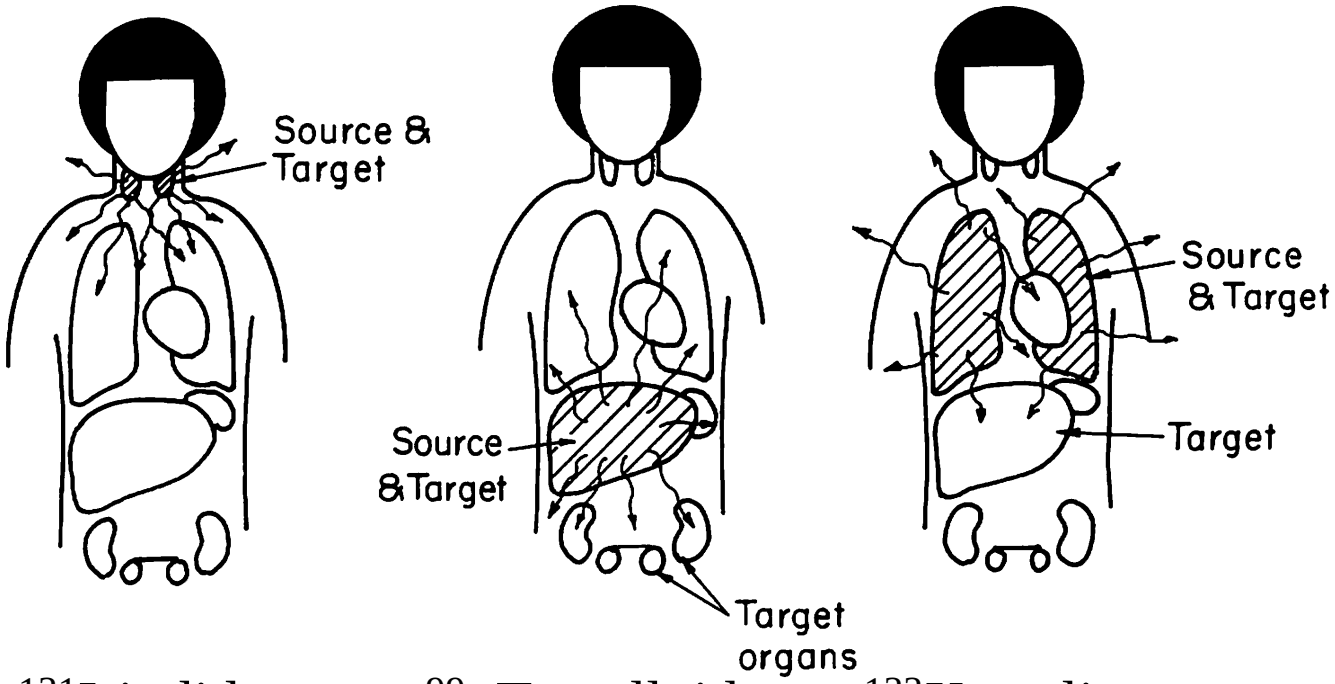

^{131}I-iodide ^{99m}Tc-colloids ^{133}Xe-saline

These examples show only one source organ

Residence time (τ)

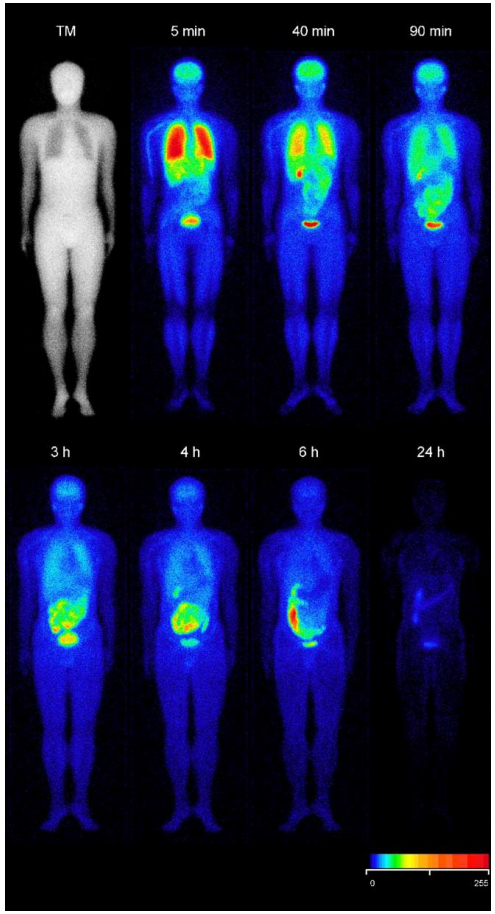

τ can be computed from whole-body biodistribution data

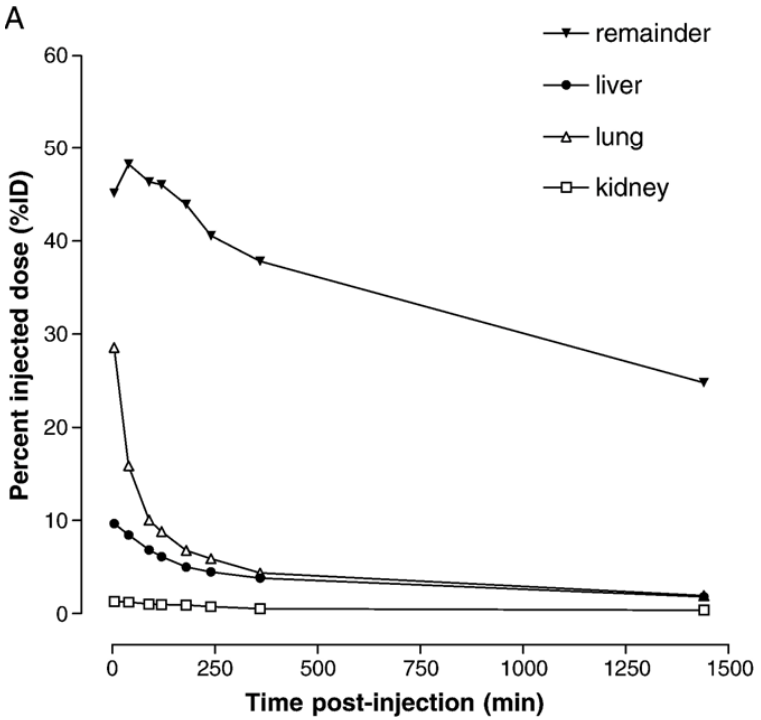

Lin KJ, et al. *Nucl Med Biol* 2006;33:193-202.

Why need internal dosimetry for a novel radiopharmaceutical?

- Balancing benefits and risks
- Interface of physician, patient and physicist

Critical organ

[^{123}I]ADAM radiation doses for adult male (mean±S.D., in microgray per megabecquerel)

Organ	Urine-voiding interval (mean±S.D.)	
	2.4 h	4.8 h
Adrenals	$1.08\times10^{-2}\pm8.54\times10^{-4}$	$1.08\times10^{-2}\pm8.33\times10^{-4}$
Brain	$1.08\times10^{-2}\pm2.32\times10^{-3}$	$1.08\times10^{-2}\pm2.32\times10^{-3}$
Breasts	$5.82\times10^{-3}\pm2.72\times10^{-4}$	$5.83\times10^{-3}\pm2.70\times10^{-4}$
Gallbladder wall	$8.35\times10^{-2}\pm3.42\times10^{-2}$	$8.36\times10^{-2}\pm3.41\times10^{-2}$
LLI wall	$5.88\times10^{-2}\pm2.76\times10^{-2}$	$6.06\times10^{-2}\pm2.74\times10^{-2}$
Small intestine	$4.03\times10^{-2}\pm3.67\times10^{-3}$	$4.09\times10^{-2}\pm3.57\times10^{-3}$
Stomach	$1.08\times10^{-2}\pm8.33\times10^{-4}$	$1.08\times10^{-2}\pm7.77\times10^{-4}$
ULI wall	$6.68\times10^{-2}\pm1.15\times10^{-2}$	$6.73\times10^{-2}\pm1.14\times10^{-2}$
Heart wall	$1.21\times10^{-2}\pm1.53\times10^{-4}$	$1.21\times10^{-2}\pm1.53\times10^{-4}$
Kidneys	$2.75\times10^{-2}\pm7.97\times10^{-3}$	$2.76\times10^{-2}\pm7.97\times10^{-3}$
Liver	$1.88\times10^{-2}\pm2.36\times10^{-3}$	$1.88\times10^{-2}\pm2.35\times10^{-3}$
Lungs	$2.91\times10^{-2}\pm1.22\times10^{-3}$	$2.91\times10^{-2}\pm1.22\times10^{-3}$
Muscle	$8.15\times10^{-3}\pm4.79\times10^{-4}$	$8.58\times10^{-3}\pm4.22\times10^{-4}$
Ovaries	$2.08\times10^{-2}\pm3.12\times10^{-3}$	$2.23\times10^{-2}\pm2.94\times10^{-3}$
Pancreas	$1.22\times10^{-2}\pm1.10\times10^{-3}$	$1.22\times10^{-2}\pm1.05\times10^{-3}$
Red marrow	$8.53\times10^{-3}\pm6.43\times10^{-4}$	$8.76\times10^{-3}\pm6.07\times10^{-4}$
Bone surfaces	$1.37\times10^{-2}\pm8.08\times10^{-4}$	$1.40\times10^{-2}\pm7.55\times10^{-4}$
Skin	$4.82\times10^{-3}\pm2.48\times10^{-4}$	$4.94\times10^{-3}\pm2.31\times10^{-4}$
Spleen	$2.61\times10^{-2}\pm3.70\times10^{-3}$	$2.61\times10^{-2}\pm3.74\times10^{-3}$
Testes	$6.91\times10^{-3}\pm2.46\times10^{-4}$	$8.02\times10^{-3}\pm1.60\times10^{-4}$
Thymus	$7.69\times10^{-3}\pm3.21\times10^{-4}$	$7.69\times10^{-3}\pm3.21\times10^{-4}$
Thyroid	$3.92\times10^{-2}\pm2.47\times10^{-2}$	$3.92\times10^{-2}\pm2.47\times10^{-2}$
Urine bladder wall	$5.14\times10^{-2}\pm5.56\times10^{-3}$	$1.00\times10^{-1}\pm1.25\times10^{-2}$
Uterus	$1.75\times10^{-2}\pm7.64\times10^{-4}$	$2.16\times10^{-2}\pm3.46\times10^{-4}$
Total body	$9.83\times10^{-3}\pm6.78\times10^{-4}$	$1.02\times10^{-2}\pm6.05\times10^{-4}$
EDE[a]	$3.02\times10^{-2}\pm5.11\times10^{-3}$	$3.37\times10^{-2}\pm4.60\times10^{-3}$
ED[a]	$2.60\times10^{-2}\pm4.04\times10^{-3}$	$2.88\times10^{-2}\pm3.96\times10^{-3}$

[a] Units for EDE and ED are millisievert per megabecquerel.

Lin KJ, et al. *Nucl Med Biol* 2006;33:193-202.

PK Data analysis

- Two organs, liver and kidney, quickly become involved in metabolism and excretion.
- The kinetics of hepatic absorption of drug are complicated by the dual blood supply from the hepatic artery (~90%) and portal vein (~10%)
- Renal processing of drug is efficient glomerular filtration from blood followed by tubular reabsorption.
- It is reported that drug X uptake by brain are reduced by both isoflurane (57%) and ketamine/xylazine (19%)
- It is reported that warming and fasting also significantly reduce drug X uptake by brown adipose tissue.
- Some drug may re-distributed after first pass (i.e. from lung…)

•. 2012 Mar;26(2):69-76
•. 2012 Mar;26(2):69-76

Drug occupancy

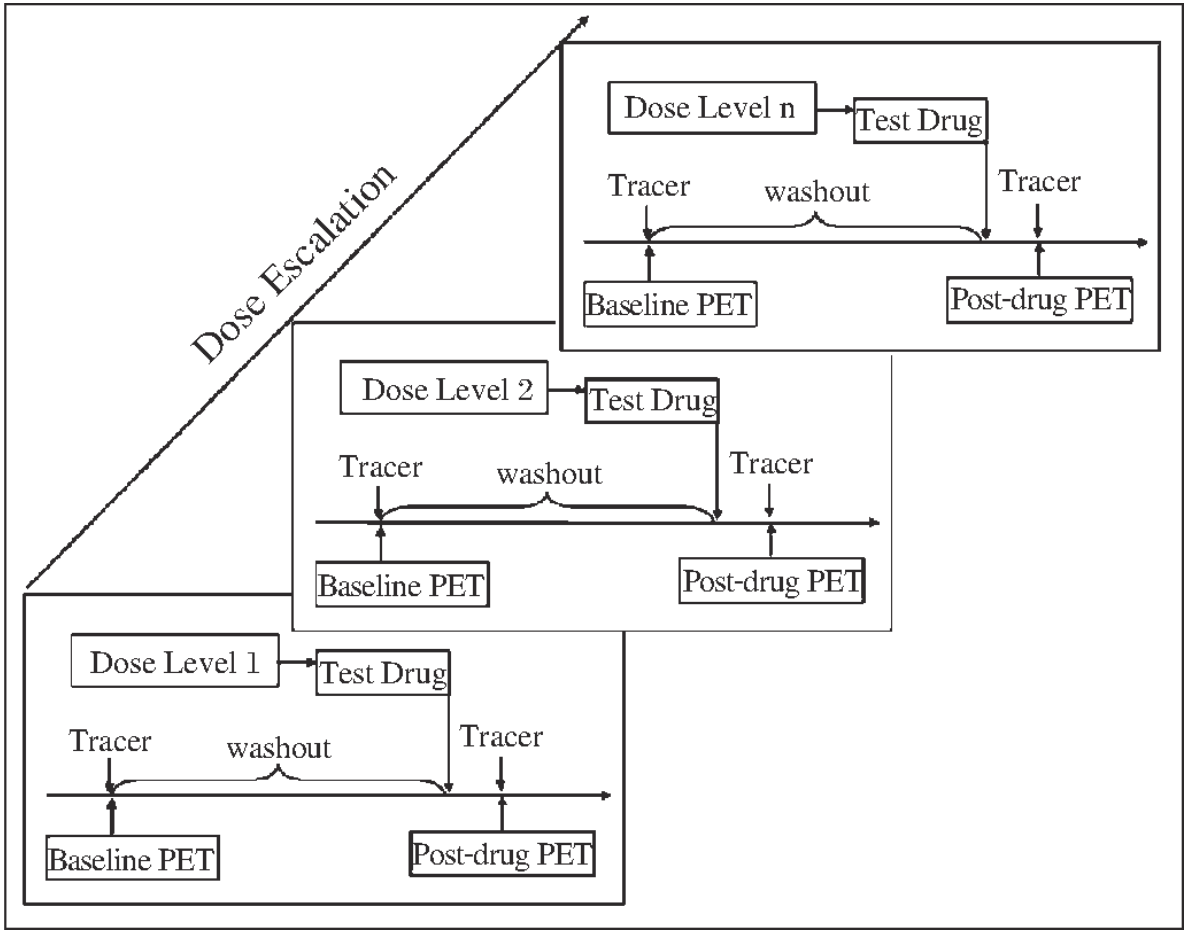

J Biomed Res. 2012 Mar;26(2):69-76.

Drug occupancy

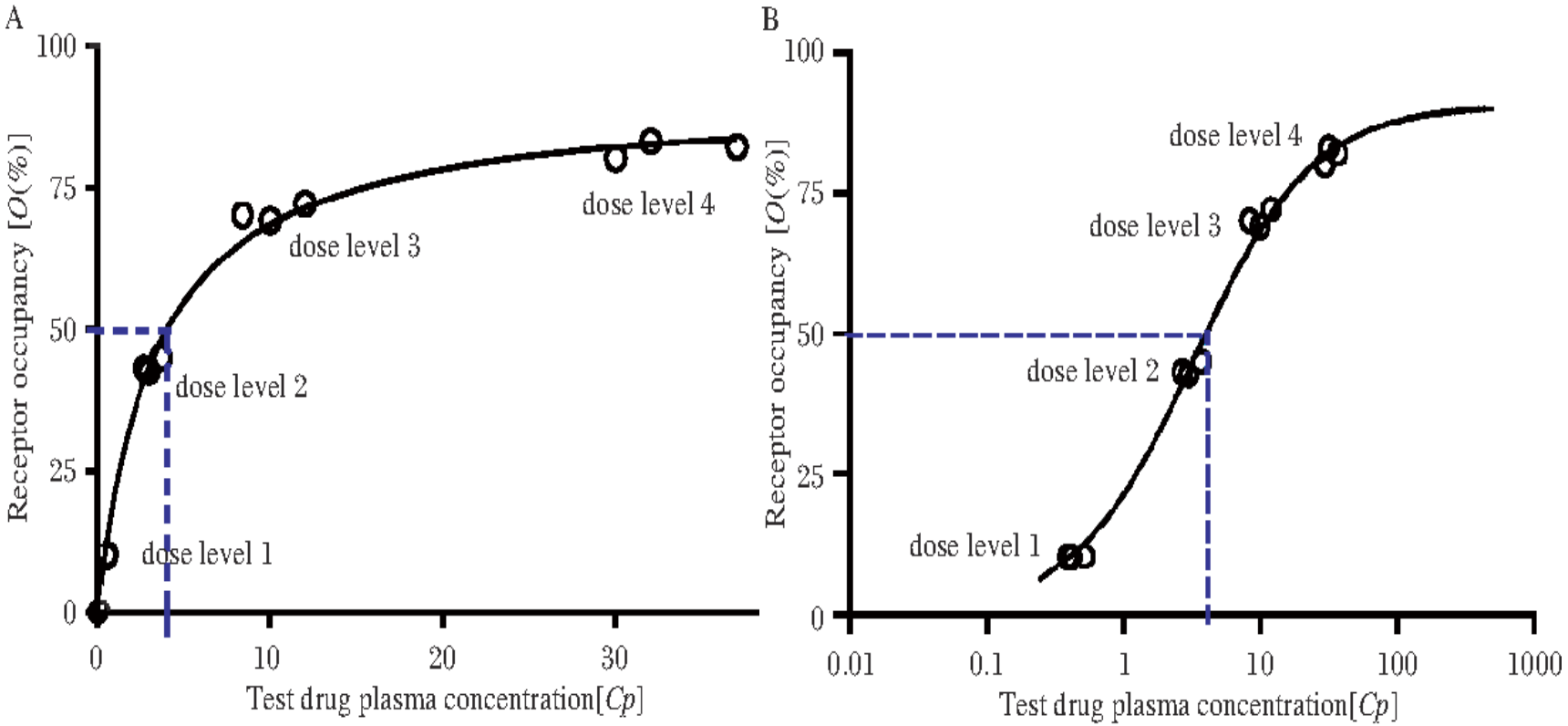

J Biomed Res. 2012 Mar;26(2):69-76.

Macroautoradiographic

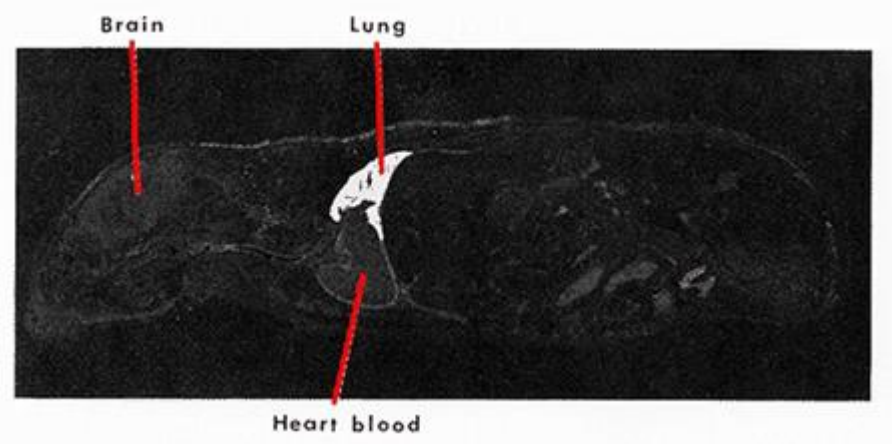

From Glenn, H. J. and Colombetti, L. G., Eds. Biologic Applications of Radiotracers. CRC Press, Inc., Boca Raton, Fl, 1982: 96. Previously from Oskarson, A. and Tjalve, H., Br. J. Ind. Med., 36, 326, 1979

Autoradiogram of a mouse 24 hr after intravenous injection of nickel carbonyl labelled with 63Ni. 鎳

- **There is a very selective accumulation in the *lung*. (The activity is localized in the alveolar, not the bronchial, part of the lung.)**
- **Nickel carbonyl and certain other nickel compounds are suspected to cause *lung cancer*.**

Neurodegeneration

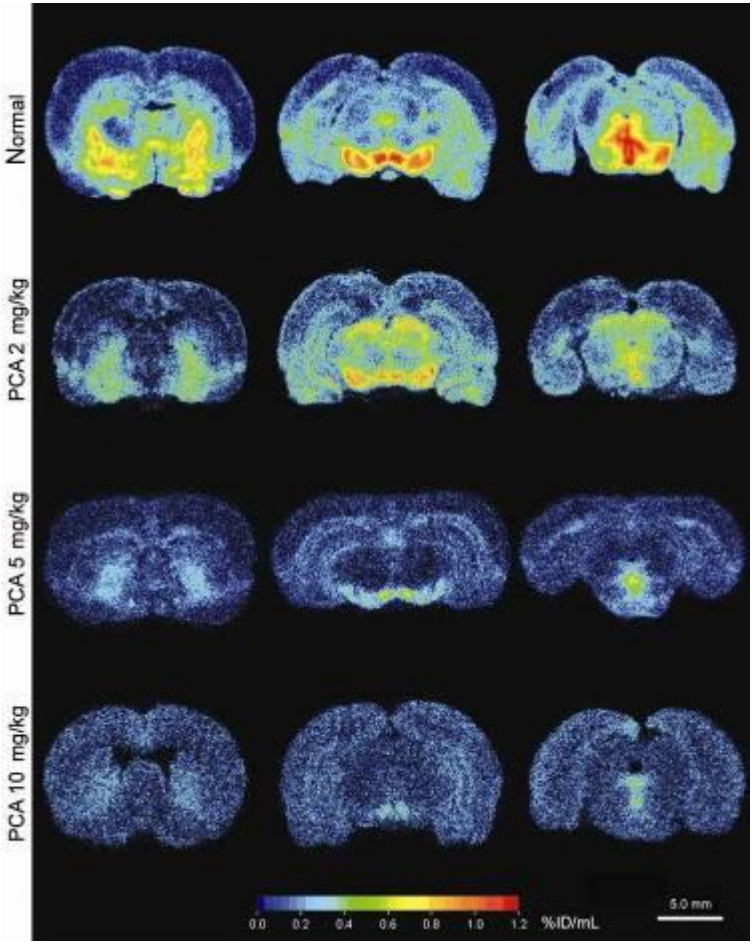

Cell migration

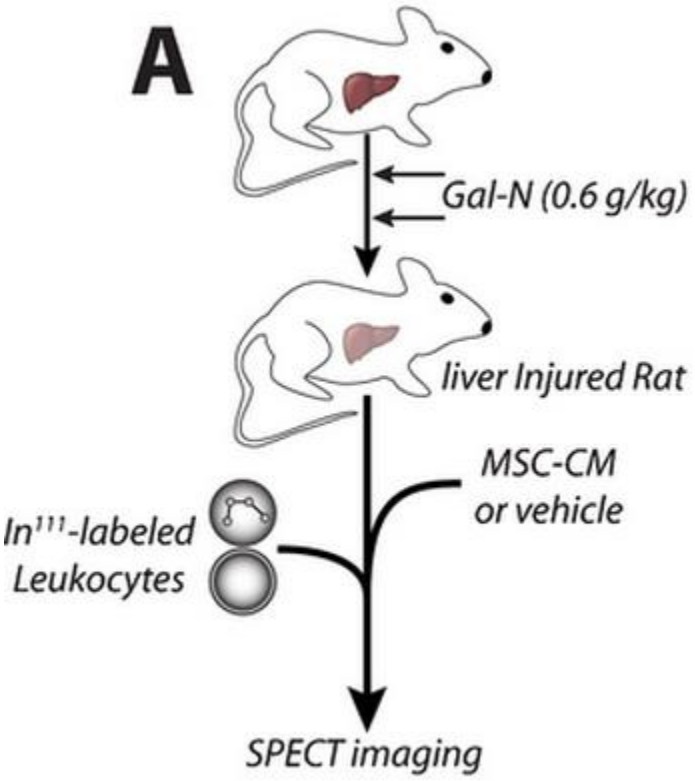

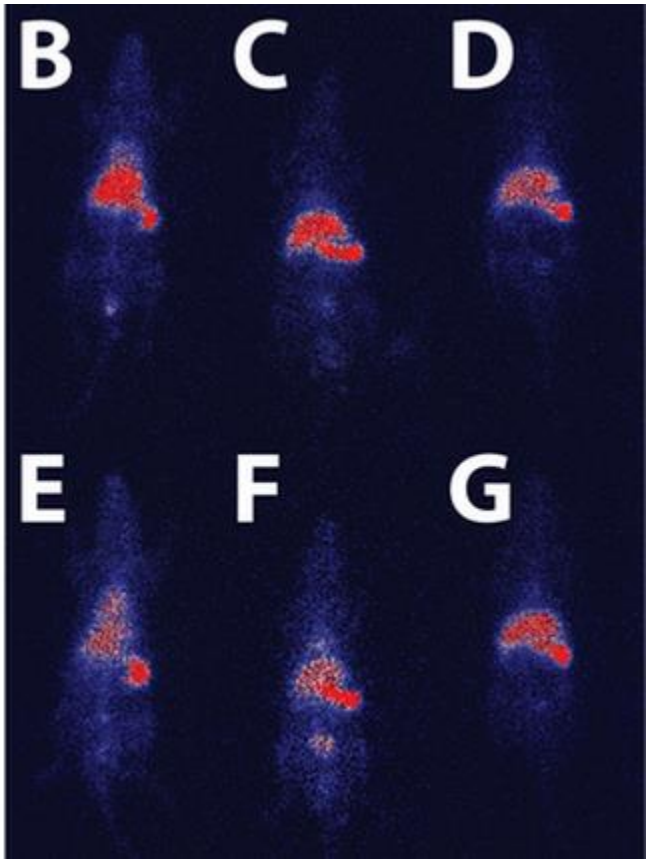

DOI: 10.1371/journal.pone.0000941

Mechanism

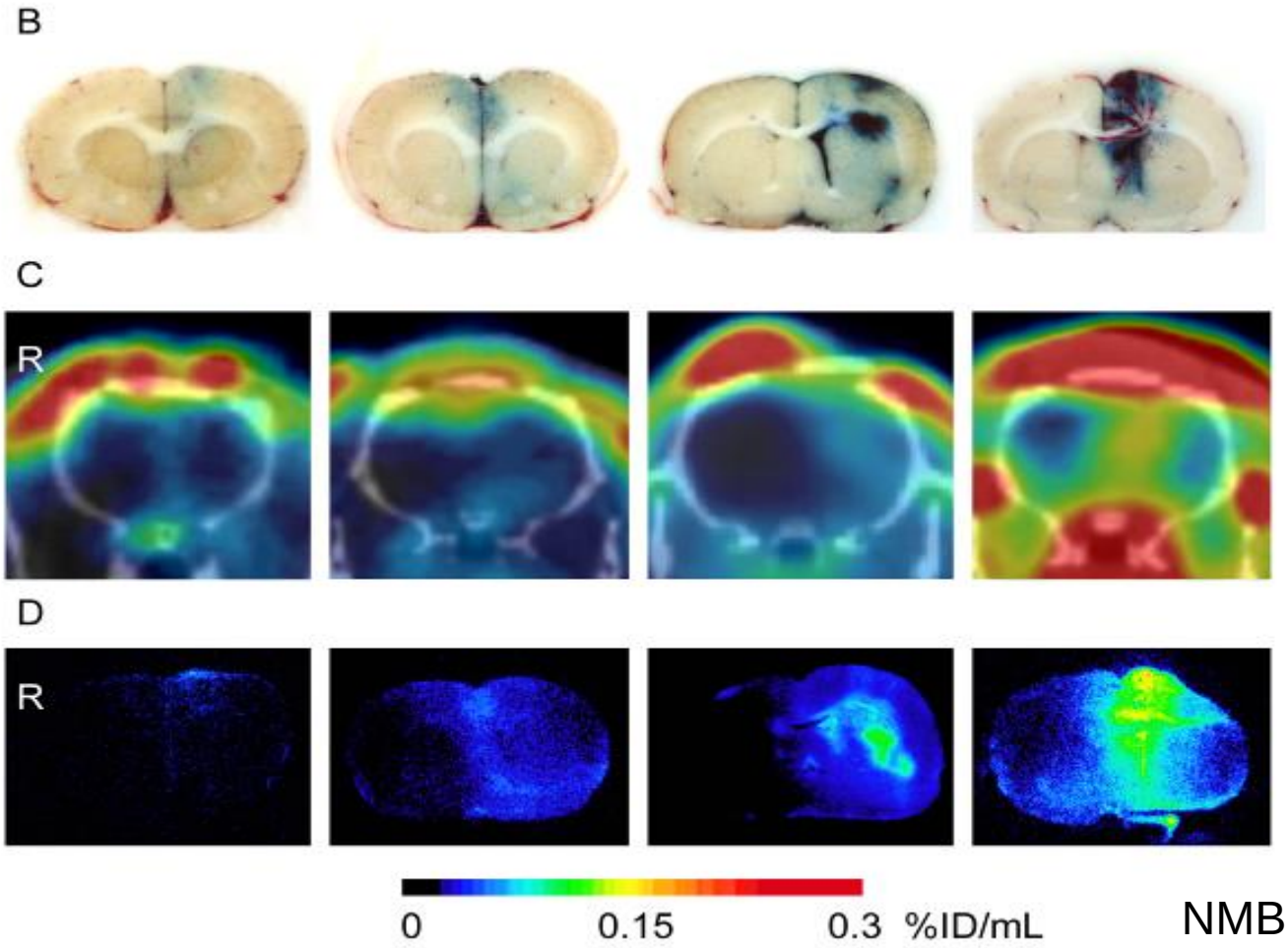

NMB 2009

Embryo-foetal transfer

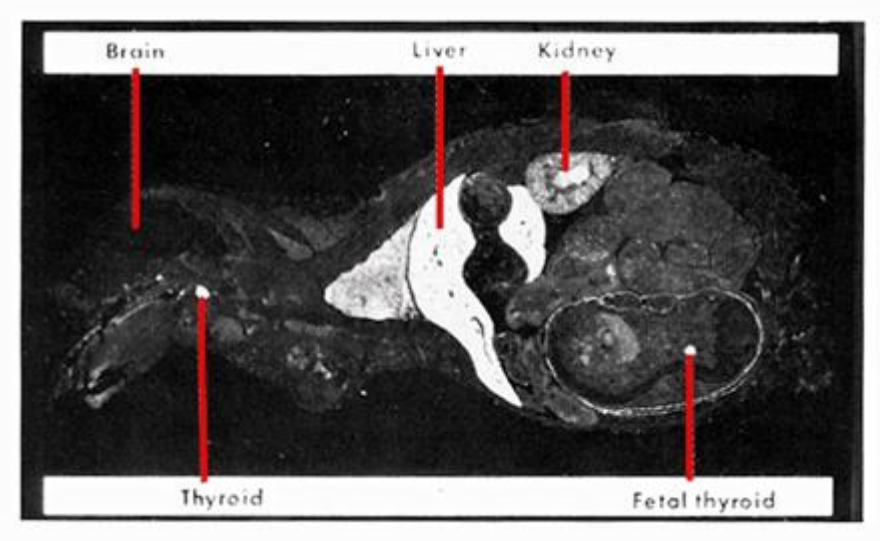

From Glenn, H. J. and Colombetti, L. G., Eds. Biologic Applications of Radiotracers. CRC Press, Inc., Boca Raton, Fl, 1982: 103

Journal of Clinical Endocrinology & Metabolism **43** (1): 152–8.

- ***C-14 Thiouracil*, which blocks the formation of iodinated thyroid hormones, is accumulated in the main site of action (thyroid gland) in both the mother and the fetus.**
- **The blocking of the formation of iodinated hormones in the fetal thyroid may stimulate the fetal pituitary to an increased production of thyrotropic hormone, which in turn may cause an extensive growth of the fetal thyroid (*fetal goiter*).**

Selection of drug candidates

0.08 h p.d.

24 h p.d.

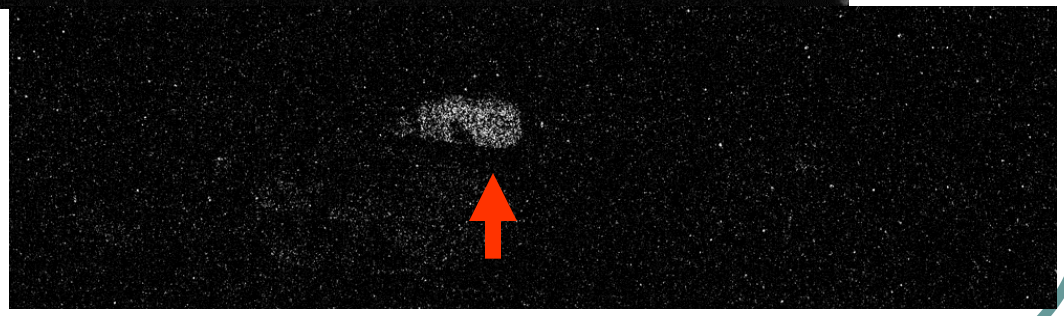

72 h p.d.

NOV123-2 : uptake / tumor / iv dosing

8.Personalized medicine

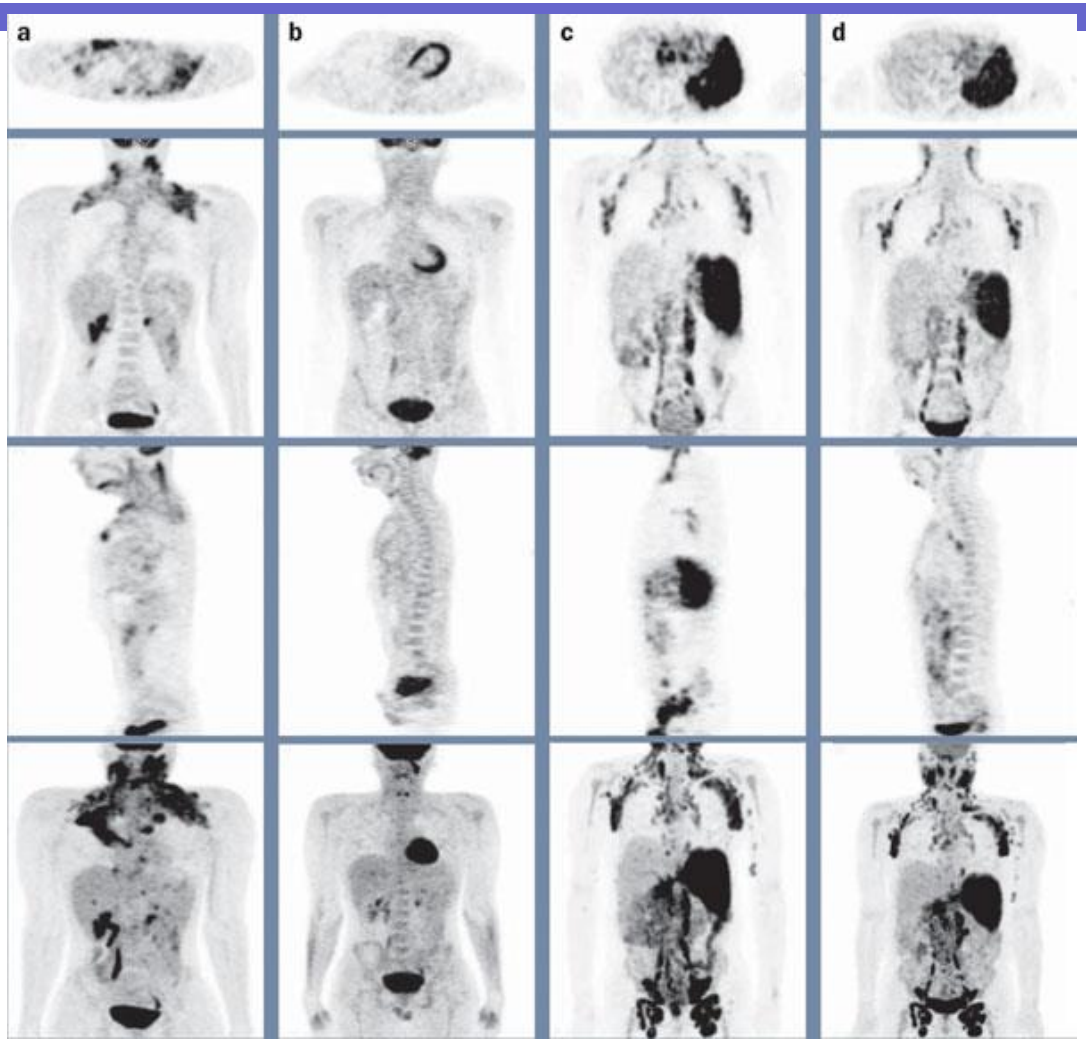

Nature Reviews Clinical Oncology **7**, 665-668 (November 2010)

Personalized medicine

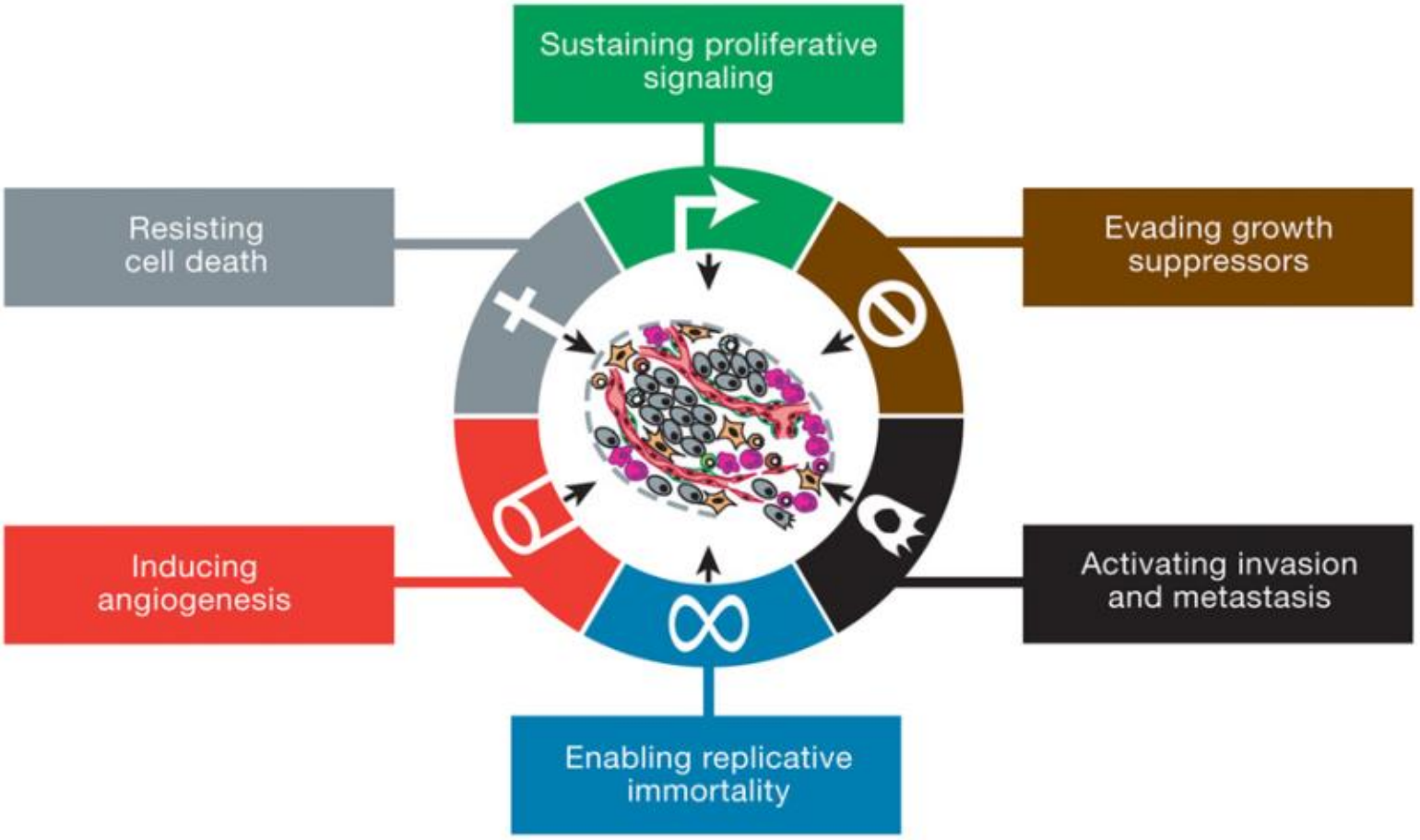

Cell. 2011 Mar 4;144(5):646-74.

Personalized medicine

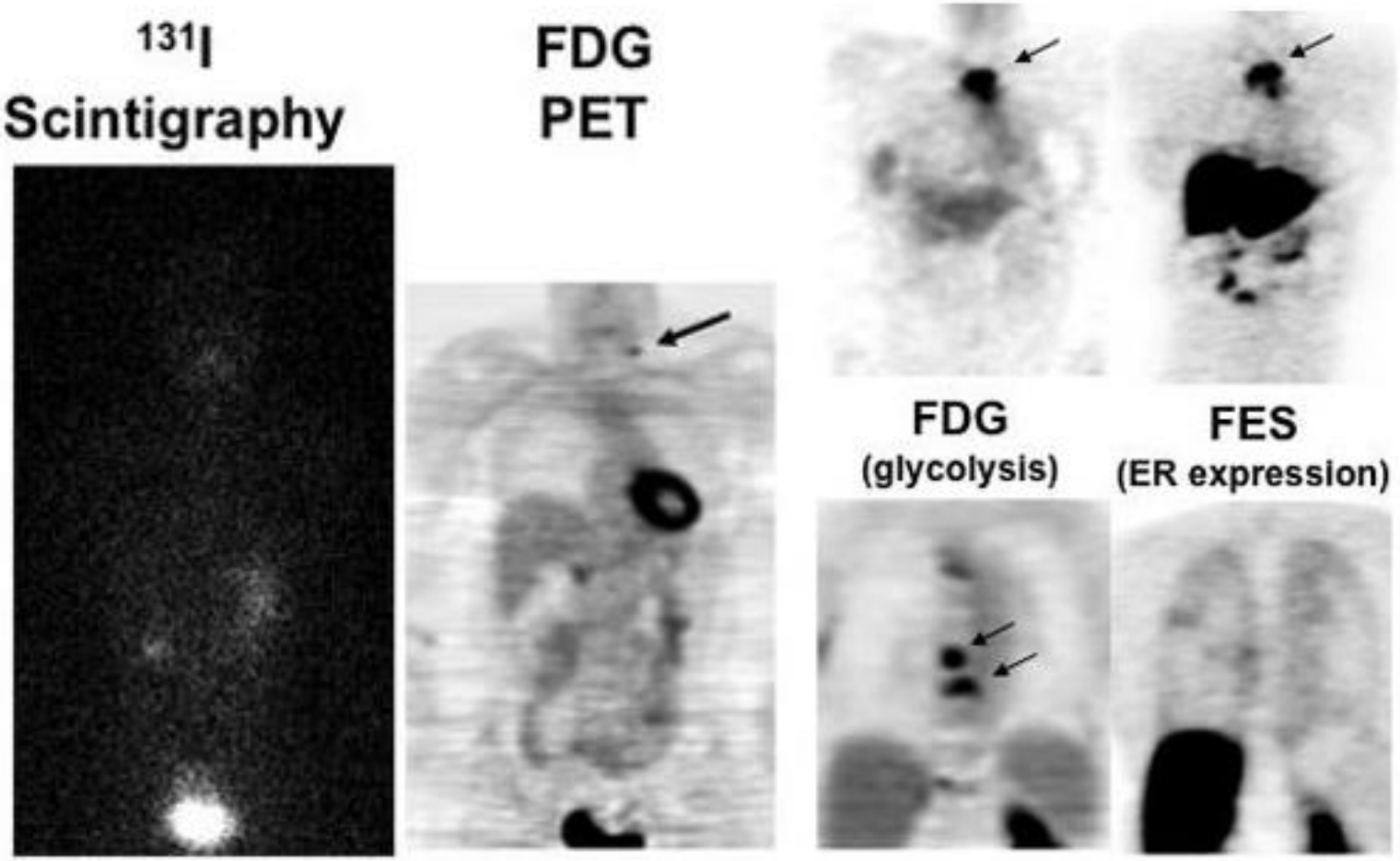

Personalized medicine

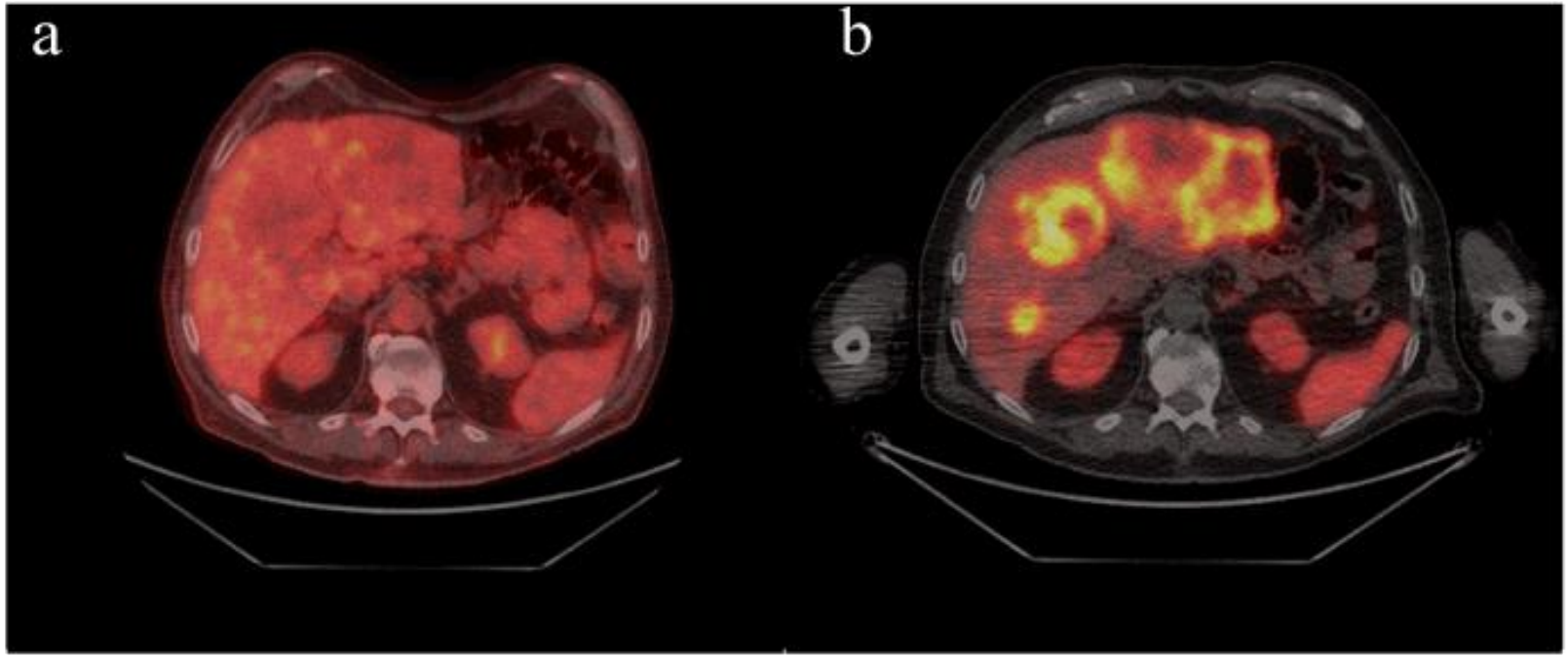

Registered axial images of patient with multiple metastases of a lowgrade neuro-endocrine tumor. FDG PET-CT (a) does not show any increased FDG ...

Personalized medicine

	Well-differentiated		Poorly differentiated
Grade (ENETS)	Low (G1)	Intermediate (G2)	High (G3)
Ki-67 index (%)	≤2	3-20	>20
Anatomic imaging	more rapid growth on serial imaging		
Functional imaging	Octreoscan SPECT or SSTR PET +ve		FDG PET +ve
Prognosis	Indolent (slowly growing)		Aggressive
Treatment options	Surgery for localised +/- resectable metastatic disease		
	Observation Somatostatin analogues Radionuclide therapy		Chemotherapy
	Everolimus, sunitnib, α-interferon Liver metastases: radiofrequency ablation, hepatic embolisation, TACE, SIR-Spheres		

Figure 1. Classification of neuroendocrine tumor with corresponding imaging features and treatment options. From Hofman *et al*., 2011. SPECT, single photon emission tomography; PET, positron emission tomography; SSTR, somatostatin receptor; TACE, transarterial chemoembolization.

Changing Paradigms with Molecular Imaging of Neuroendocrine Tumors
Discovery Medicine

Personalized medicine

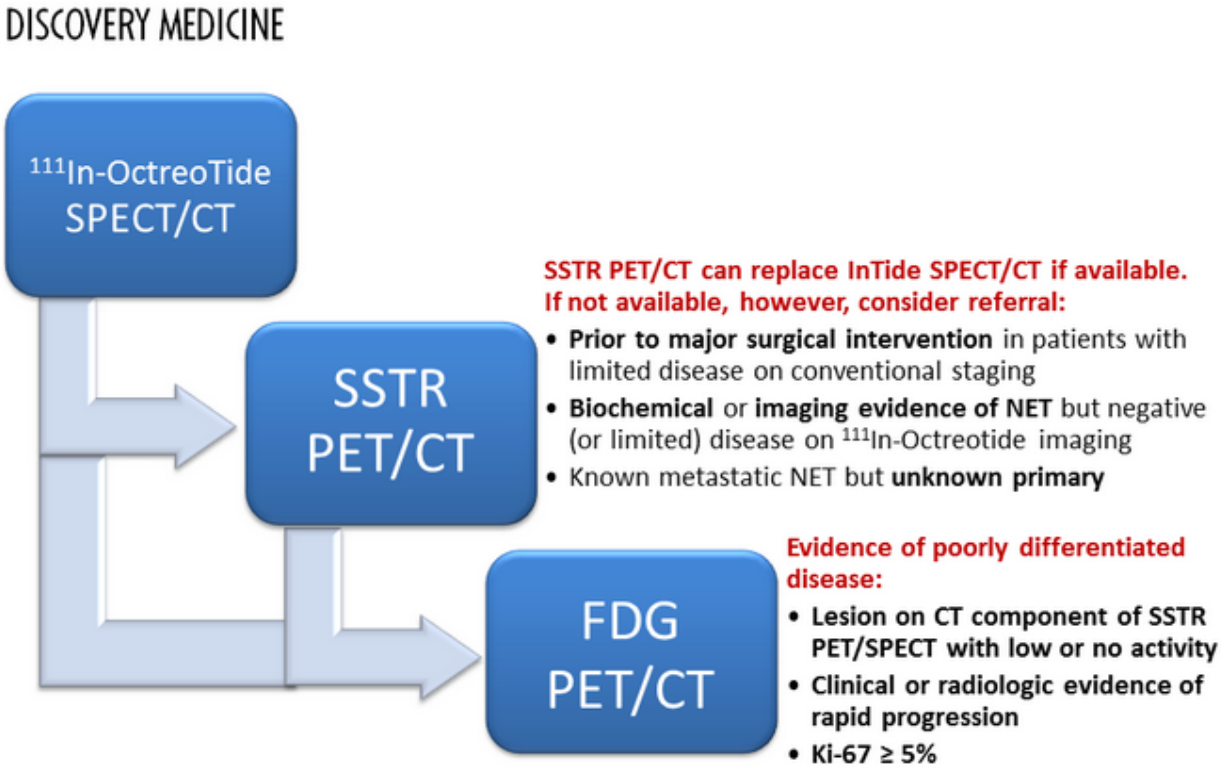

Figure 3. Suggested molecular imaging pathway. SSTR PET/CT: somatostatin receptor positron emission tomography/computed tomography. Includes Ga-68 DOTA-TATE (GaTate), DOTA-TOC (GaToc), and DOTA-NOC (GaNoc) PET/CT.

Changing Paradigms with Molecular Imaging of Neuroendocrine Tumors
Discovery Medicine

Personalized medicine

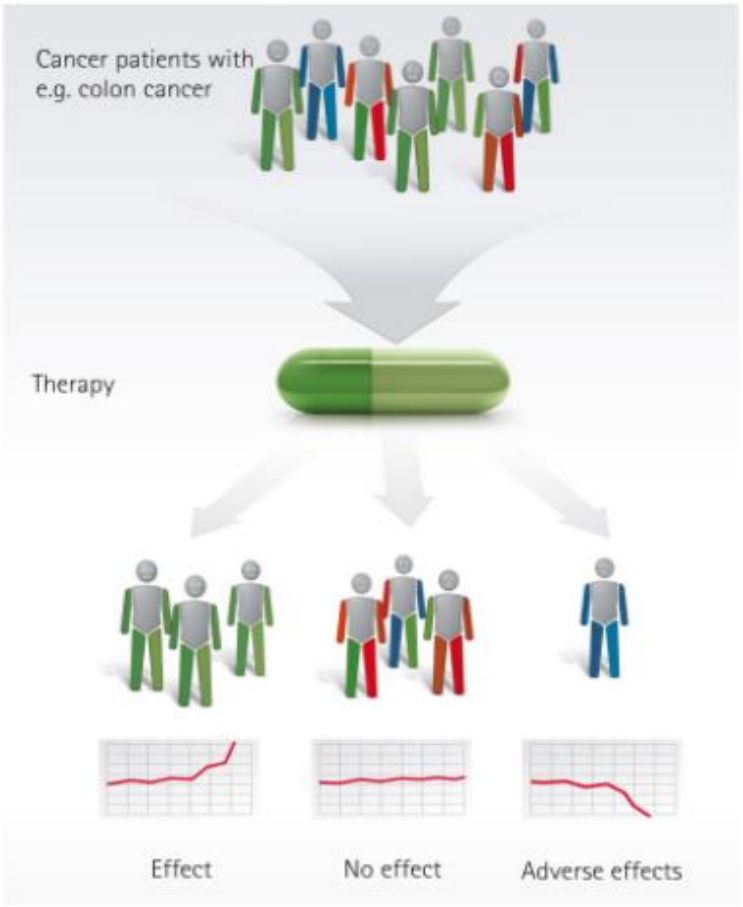

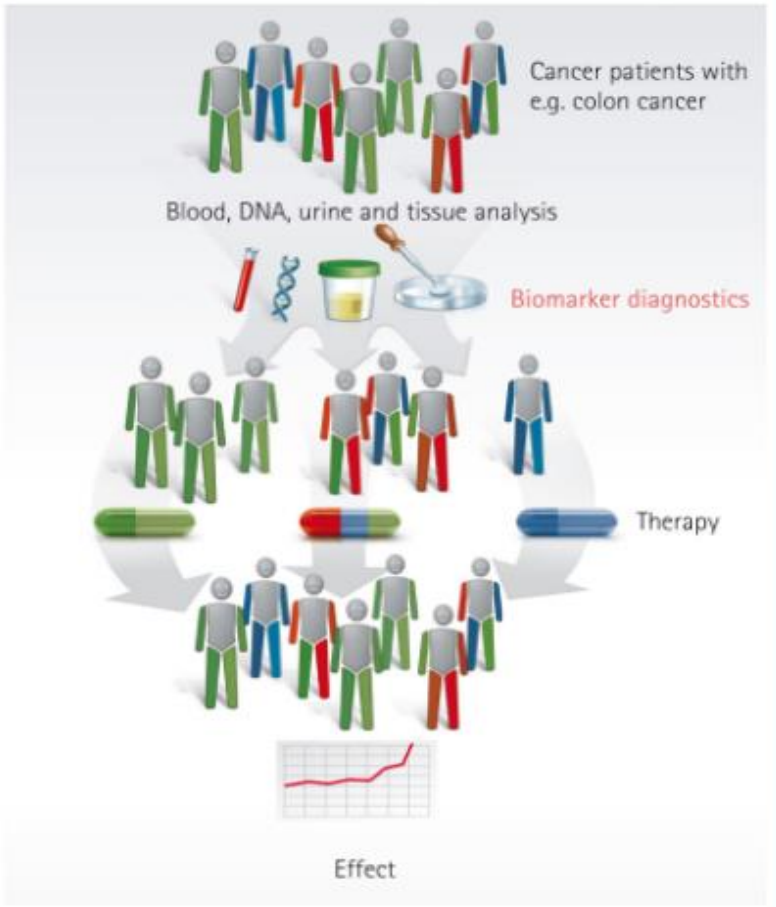

Renub Research June 13, 2013

Take home message

- 藥物動力學 Pharmacokinetics (PK)

  描述隨著時間藥物在進到生物體內的狀況，特別是從血液中的清除 clearance from blood ，或是初級代謝 first pass metabolism

- 從生物分佈及藥物動力學可知

  輻射劑量學，診斷評估，治療評估，毒理評估